REDUCTION OF PROPELLER VIBRATION AND CAVITATION BY CYCLIC VARIATION OF BLADE PITCH

by

Stuart Dodge Jessup

SUBMITTED IN PARTIAL FULFILLMENT

OF THE REQUIREMENTS FOR THE

DEGREE OF MASTER IN SCIENCE IN

OCEAN ENGINEERING

at the

Massachusetts Institute of Technology

May, 1976

Signature of Author . . . . . .
Department of Ocean Engineering

Certified by . . . . . .
Thesis Supervisor

Accepted by . . . . . .
Chairman, Departmental Committee on Graduate Students

REDUCTION OF PROPELLER VIBRATION AND CAVITATION BY CYCLIC VARIATION OF BLADE PITCH

by

Stuart Dodge Jessup

Submitted to the Department of Ocean Engineering on May 21, 1976 in partial fulfillment of the Requirements for the Degree of Master in Science in Ocean Engineering.

ABSTRACT

An experiment was conducted to demonstrate the reduction of propeller vibration and cavitation by the cyclic variation of blade pitch. The pitch of one blade on a five-bladed model propeller was cyclically varied to maintain constant angle of attack in a spatially nonuniform wake. The degree of transient cavitation was compared on the fixed and oscillating blades at various operating conditions. From this, an estimation was made of the reduction in the variation of blade angle of attack due to blade pitch variation. The results were correlated with an approximate unsteady lifting line analysis.

THESIS SUPERVISOR: Justin E. Kerwin

TITLE: Professor of Naval Architecture

ACKNOWLEDGEMENTS

No part of the experiment could have been completed without the aid of many individuals. Initially, Dr. Junger presented the problem to me, and provided support throughout the project. The Bird-Johnson Company and the NSDRC agreed to the use of the hub and the blades. The Mechanical Engineering Machine Shop performed most of the machining for the blade mechanism. Mr. Dean Lewis assisted in the tests in the Propeller Tunnel. Finally, Professor Justin Kerwin provided direction and advice in a field that was new to me. I wish to thank all of these individuals for their support to bring my project to completion.

TABLE OF CONTENTS

LIST OF FIGURES

LIST OF TABLES

LIST OF SYMBOLS

V_S = Speed of the ship

V_a = Inflow Velocity to Propeller

β = Advance Angle

$= \tan^{-1}\left[\frac{V_a}{r\omega}\right]$

ϕ_Θ = Pitch Angle

J = Advance Coefficient

$= \frac{V_a}{ND}$

V_T = Tunnel Velocity Ahead of the Wake Screen

V_{max} = Inflow Velocity at .7 Radius in the Maximum Wake Region

V_{min} = Inflow Velocity at .7 Radius in the Minimum Wake Region

V_{AVE} = Average Inflow Velocity at .7 Radius

J_{min} = $\frac{P_T - P_V}{\frac{1}{2}P\left[(.7R_O\omega)^2 + (V_{min})^2\right]}$

= Blade Cavitation Number in the Minimum Wake Region at the .7 Radius

J_{max} = Blade Cavitation Number in the Maximum Wake Region at the .7 Radius

= $\frac{P_T - P_V}{\frac{1}{2}P\left[(.7R_O\omega)^2 + (V_{max})^2\right]}$

P_T = Static Tunnel Pressure

P_V = Vapor Pressure

J' = Advance Coefficient Used in Spindle Torque Test

$$= \frac{V_{AVE}}{\sqrt{V_{AVE} + n^2D^2}}$$

D = Diameter of the Model Propeller

R_o = Radius of the Model Propeller

ω = Angular Velocity of Propeller Rotation (rad/sec)

n = Angular Velocity of Propeller Rotation (cycles/sec)

T = Measured Thrust

$\frac{q}{V}$ = Net Perturbation Velocity at a Position of the Blade Section

$\frac{\Delta v}{V}$ = Perturbation Velocity Due to Camber at Ideal Angle of Attack

$\frac{v}{V}$ = Perturbation Velocity Due to Thickness

$\frac{\Delta v_a}{V}$ = Perturbation Velocity Due to Angle of Attack, Per Unit Lift Coefficient

α_i = Ideal Angle of Attack

C_{Li} = Lift Coefficient at the Ideal Angle of Attack

α_{2D} = 2-D Sectional Angle of Attack

α_{3D} = Corrected 3-D Angle of Attack

$\Delta\alpha$ = Variation in Angle of Attack

α_{max} = Maximum Angle of Attack, Occuring in the Wake Region

α_{min} = Minimum Angle of Attack, Occuring in the Wake Region

β_i = Hydrodynamic Advance Angle

$$= \tan^{-1}\left(\frac{V_a + v_a^*}{w_r + v_t^*}\right)$$

v_a^* = Axial Induced Velocity

v_t^* = Tangential Induced Velocity

$\Delta\Phi$ = Pitch Angle Variation

1. Introduction

The operation of a propeller in a nonuniform wake is a major source of ship vibration. The volume of water flowing into the propeller, referred to as the wake, often has an irregular velocity profile due to the shape of the hull ahead of the propeller. The velocity of the incoming wake on each blade of the propeller will vary according to its position. As the blade rotates, it will be subjected to a cyclically varying inflow velocity, which when summed with the propeller's angular velocity, produces a cyclically varying angle of attack on the individual blades. Therefore each blade experiences a similarly varying lift and drag. In the propeller's frame, this corresponds to cyclically varying thrust, torque, and transverse forces.

In recent years, modulated propeller forces caused by this effect have become severe on commercial ships. Due to the increase in size of these ships larger propulsion systems have led to an increase in the magnitude of propeller induced vibration. Also, the trend towards fuller sterns, to increase cargo capacity, has led to more extreme wakes and further increased vibratory forces.

Aside from the vibration problem, cyclic variations in angle of attack of the blades can lower the effective cavitation threshold associated with propeller operation

in uniform flow. To prevent this form of cavitation, the designer often reaches a less than optimal design, sacrificing a reduction in speed or efficiency. If cavitation does occur, it forms in a transient fashion. Sheet cavitation will grow in the extreme parts of the wake and collapse upon entering the mild wake regions. This results in pitting of the blade surfaces, extreme radiated noise, and a decrease in propeller efficiency.

The cavitation problem is most severe for naval ships. With requirements of maximum speed and mininum radiated noise, irregular wake conditions greatly disadvantage those goals by lowering the cavitation threshold.

An obvious way of reducing this form of propeller induced vibration is to provide a more uniform wake. This is done on naval ships by placing the propellers under the hull. A slight wake is produced by the angle the propeller shaft forms with the free stream. A faired stern section would also reduce the problem, but is not often considered justified in the overall design.

Large modulated thrust and torque components occur when wake harmonics exist that are multiples of the propeller blade number. The wakes of most surface ships, and submersibles, because they are symetrical about their vertical axis, have dominant, even harmonic wake representations. By

using an odd number of blades, variations in thrust and torque can be reduced. Unfortunately, modulated transverse forces occur when multiples of the blade number equal the wake harmonic number plus or minus one. So an odd number of blades would tend to increase transverse forces. Proper blade number selection can reduce certain vibratory forces, while enhancing others. In some design situations, this could be beneficial, but the problem of transient cavitation still exists.

Propellers with large numbers of blades, for example seven, would induce vibration only at high harmonics of the wake. Magnitudes of the higher harmonics, sixth, seventh, and larger, are usually relatively small, so both transverse force, and thrust and torque variations could be reduced. Again, cavitation would not be effected.

Propellers with extremely skewed blades cause the local velocity variations to be averaged out over the blade. This greatly reduces vibration, and partially reduces cavitation.

Finally, various mechanical and hydraulic devices have been designed to reduce propeller induced vibration. The vibration reducer is a hydraulic device aimed at isolating the thrust block from the modulated thrust, while transmitting the steady thrust. Another device was designed to reduce transverse vertical forces by adjustable rotating

counterweights, turned to balance out the induced propeller force. the first of these devices operates to a marginal capacity, while the second has never been tested.

All of the above methods reduce some of the modulated force components to an extent. Only one method partially reduces the transient cavitation caused by the irregular wake.

The method proposed here is the cyclic variation of blade pitch to compensate for the irregular wake. Conceptually, this method could totally reduce the modulated force components and eliminate the transient cavitation.

2. Cyclically Varying Blade Pitch -- A Solution

A conceptually simple method of reducing propeller vibration is the cyclic variation of blade pitch to maintain constant angle of attack of each blade as it rotates. Ideally, modulated thrust and torque, transverse forces, and transient cavitation could be eliminated.

Maintaining constant angle of attack of each blade is a rather general statement. Because of the variation of velocity radially in the wake, constant angle of attack could not be maintained over the entire blade. One approximation would be to design for constant angle of attack at an average spanwise position, e.g. 70% of the radius of the blade. Variation in angle of attack would occur at other parts of the blade, but would approximately average out to produce low modulated forces. A more exact method would involve using unsteady propeller theory to obtain accurate solutions for the unsteady forces, assuming a certain pitch variation. An iterative procedure could be used to minimize modulated forces with an optimum pitch variation.

The biggest drawback of this solution is its practicality as a full-scale working system. A reliable mechanism for independently articulating blades of a propeller was

perhaps the biggest deterent preventing previous development of this device. The mechanism must withstand the forces generated by the oscillatory accelerations of the blades, their added mass, and the mechanism itself. The mechanism must also withstand off design loads, such as a full stop condition, or sharp turns. Present technology developed for controllable pitch propellers could be applied to solve the problems of a cyclically varying pitch propeller.

It is the purpose of this study to show in an elementary manner that the approximate principle works. Hopefully, the next step would be to consider the possibility of a reliable, reasonable hub mechanism. Finally, an experimental and theoretical optimization study of the pitch variation could be conducted.

3. The Experiment -- General Description

It was desirable to conduct an experiment to demonstrate the basic principle of maintaining constant angle of attack to reduce modulated forces. A rigorous experiment would involve a propeller hub with all its blades capable of articulation independently. Force measuring devices would be necessary to record thrust and torque at the hub, and perhaps stresses on the individual blades. Because of the inavailability of such a model hub, and the great expense of manufacturing the device, an alternate experiment was proposed.

Existing and available was a controllable pitch five-bladed model, with one of the blades mounted on low friction ball bearings. The hub, owned by Bird-Johnson Company, was previosuly used to measure spindle torque on the bearing mounted blade under various operating conditions. A small lever arm attached to the movable spindle extended out through a center hole in the hub.

The experiment would involve a mechanism attached to the front of the hub, that would oscillate the pitch of the single blade as it rotates. The oscillations could be matched to a prescribed test wake to produce a constant

angle of attack for the average portion of the blade. The other four blades would remain at constant pitch, and be subjected to the adverse wake.

Reduction in vibration could only be related to the difference in transient cavitation on the fixed and moving blades. Ideally no cavitation would occur on the moving blade at its designed operating condition. By comparing the degree of transient cavitation on the fixed and moving blades, a rough determination of their variation in angle of attack could be obtained. Because angle of attack variations are directly related to variations in blade lift, conclusions could be made as to the reduction in propeller induced vibration.

4. Test Wake

The simulated wake used in the model test was typical of a large single screw bulk carrier. The wake was produced by a varying mesh screen positioned upstream of the propeller. For the model propeller size a maximum reduction in inflow velocity of 60% occurred at the 70% radius of the blades, at regions above and below the propeller axis. (Figure 1).

Plotting the inflow velocity versus circumferential angle, ϕ, a sinusoidal velocity of frequency twice that of the shaft frequency, summed with a mean velocity, closely approximated the wake profile. (Figure 2). Restated, the wake was modelled as only a mean velocity, and the second harmonic component. Assuming this simple wake distribution, simplified the oscillating mechanism design.

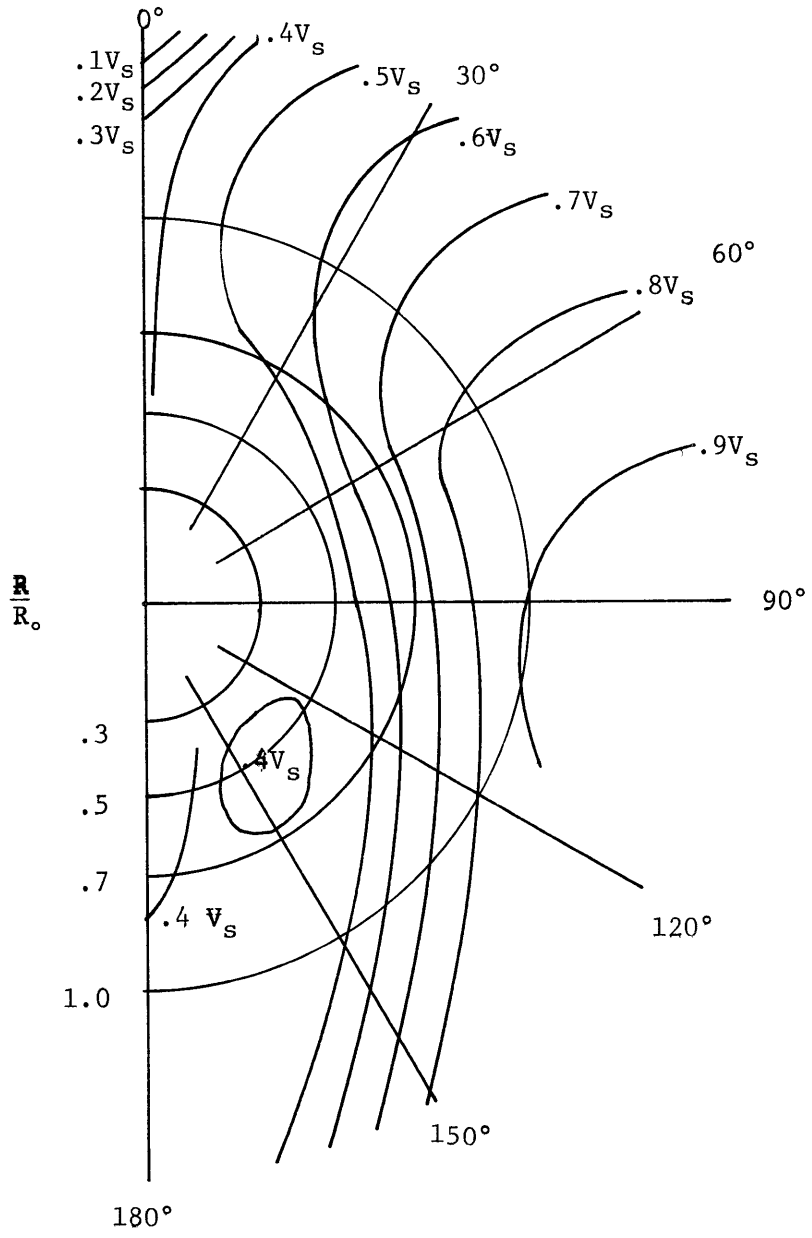

FIGURE 1 PROFILE OF WAKE SCREEN

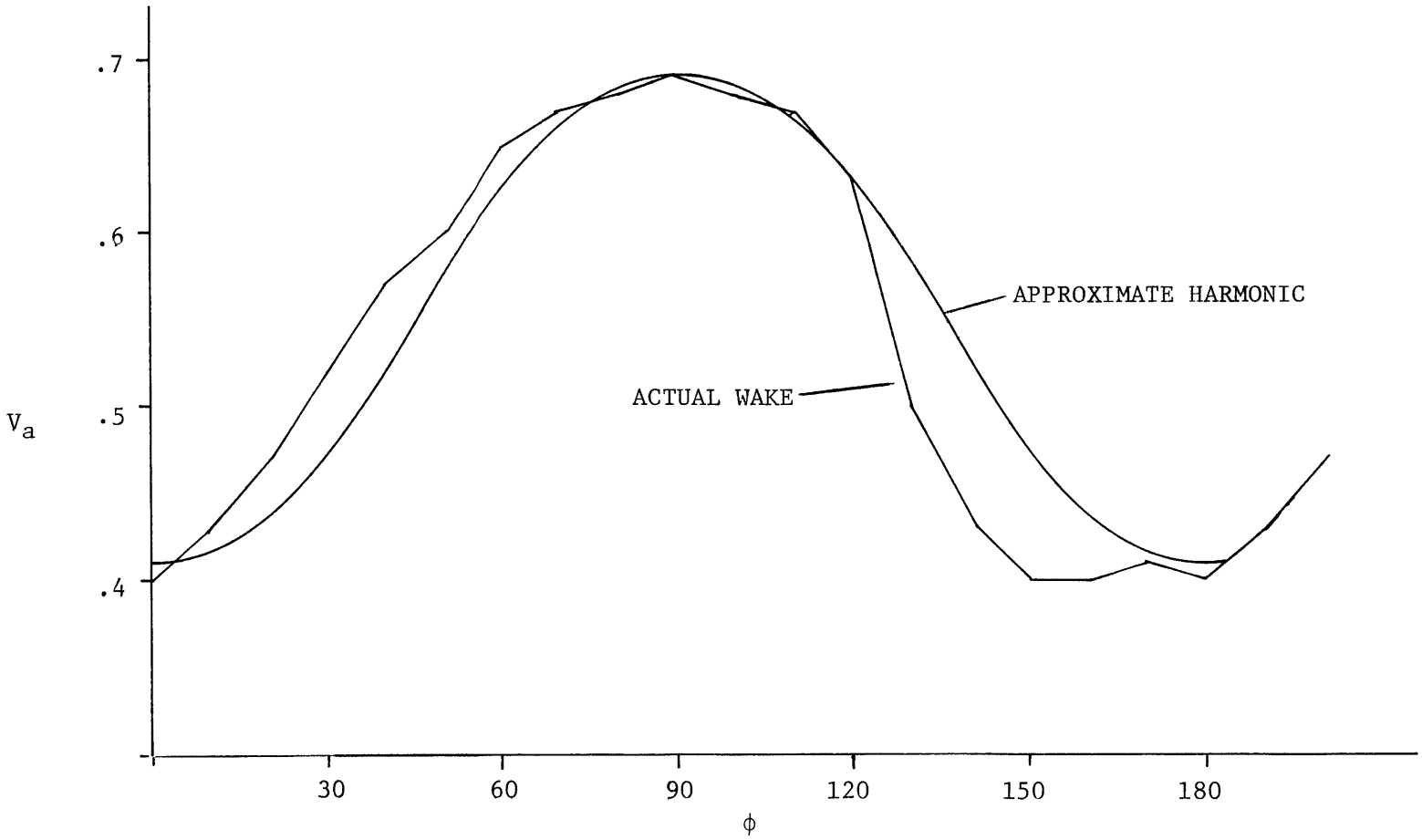

FIGURE 2 HARMONIC APPROXIMATION OF WAKE

5. Determination of Blade Pitch Variation

Before the oscillating mechanism could be designed, the magnitude of blade pitch fluctuation had to be determined. As an approximation, the necessary pitch variation depended solely on the shaft speed and the maximum and minimum wake velocity at the .7 radius position. All unsteady effects and induced velocities were neglected. As stated earlier, the angle of attack at the .7 radius was to be constant. ($\alpha_1 = \alpha_2$ in Figure 3). From Figure 3, for this to be true, the peak-to-peak pitch variation, $\Delta\Phi$, must equal $\Delta\beta$, the variation in advance angle.

It is evident from the figure, that $\Delta\Phi$ is dependent on the inflow velocity, and the shaft speed. $\Delta\Phi$ was calculated for a variety of values of J, the advance coefficient, and it was observed that for increasing values of J, $\Delta\Phi$ increased. The operating condition of the propeller was set at $J \approx 1$, which correspended to $\Delta\Phi = 9.19°$. Practical limitations within the model hub restricted $\Delta\Phi$ to a value below this assumed operating condition, as discussed in the next section.

It should be noted that the propeller type and design, J, were not typical for the wake used in the test. The experiment was not intended to model an actual ship, but to

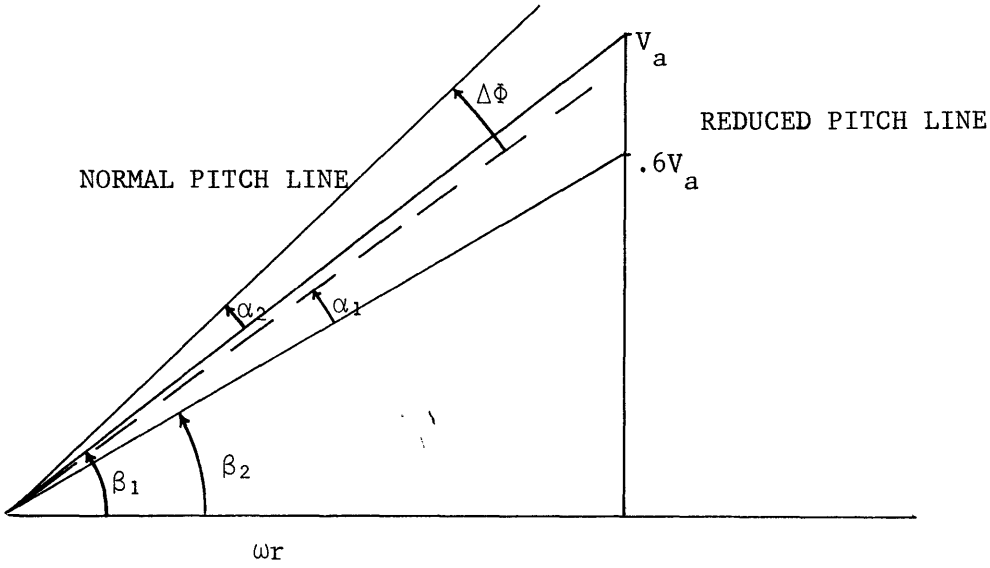

$\beta_1 - \beta_2 = \Delta\beta \sim \Delta\Phi$, PITCH ANGLE VARIATION

r= .7 of TOTAL RADIUS, R_0

V_a = MAXIMUM INFLOW VELOCITY AT r

$\Delta\beta = TAN^{-1}(.455J) - TAN^{-1}(.273J)$, where $J = V_{a/2NR_0}$

J	$\Delta\Phi$
1.0	9.2°
.9	8.5°
.8	7.7°
.7	6.8°
.6	6.0°
.5	5.0°

FIGURE 3 GEOMETRIC INTERPRETATION OF PITCH VARIATION

only provide conditions to test the concept. Because of this, maintaining the design, J, of the propeller was not necessary but provided a guideline for the design.

6. Design of Mechanism

As described earlier, the propeller hub assembly consisted of one blade mounted in an internal bearing arrangement. Extending from the internal bearing, out through a central hole in the front of the hub, was a small lever arm, referred to as the tiller. Translational motion of the end of the tiller corresponded to angular rotation of the bearing mounted propeller blade. The maximum travel of the tiller was .29" corresponding to 8° maximum angular travel of the blade. Avoiding hub modifications, this limited the maximum pitch variation.

The method of oscillating the tiller as the propeller rotated was designed. The eventual mechanism consisted of a brass assembly attached to the front of the hub. A ¼" diameter pin (cam follower) extended from the tiller, radially out through the front assembly. As the blade oscillated, the pin would oscillate radially through the front assembly. Surrounding the front assembly, a ring cam with a varying inner radius was fixed, aligned over the cam follower. The cam follower rode against the cam as the propeller rotated. A small roller bearing was mounted on the end of the cam follower to reduce frictional forces on the cam surface. The tiller and cam follower were held against the cam by a compression spring mounted on the tiller face opposite the

cam follower. The ring cam was positioned and restrained from rotating by a split collar, mated against the stationary propeller shaft casing. The front of the brass assembly was fixed to the propeller shaft through a tapered sleeve and an axially mounted allen head bolt. Figure 4 and 5 show side and front sectional views of the mechanism. Figure 6 displays the individual components of the hub and assembly.

As the propeller hub rotated, the cam follower, and thus the tiller, followed the prescribed interior shape of the ring cam. The motion of tiller would be transferred to angular variations in the single moving blade.

A main area of concern in the design was excessive wear due to high loadings at high RPM's. To minimize the outside diameter of the oscillating mechanism, and maintain reasonable thickness of the ring cam and collar, a maximum tiller travel of .26" was allowable, producing a maximum $\Delta\Phi=7.16°$

With maximum tiller travel known, the maximum force due to sinusoidal acceleration was determined. Due to the second harmonic representation of the wake, a maximum shaft frequency of 900 RPM corresponded to a mechanism fequency of 1800 RPM. Given frequency, amplitude and mass estimates of the moving parts, an inertial force of 5 lbs. was estimated. Accounting for added mass and a safety factor, the estimate was doubled for design purposes.

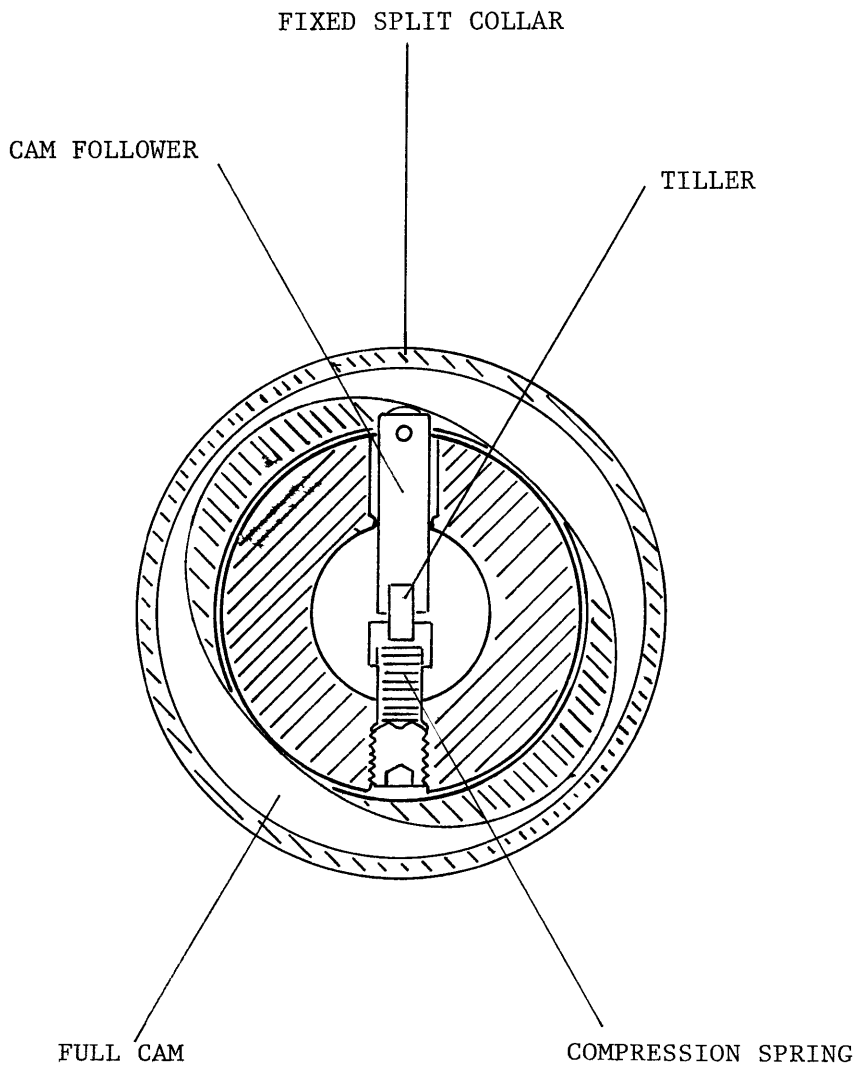

FIGURE 4 FRONT SECTIONAL VIEW OF OSCILLATING MECHANISM

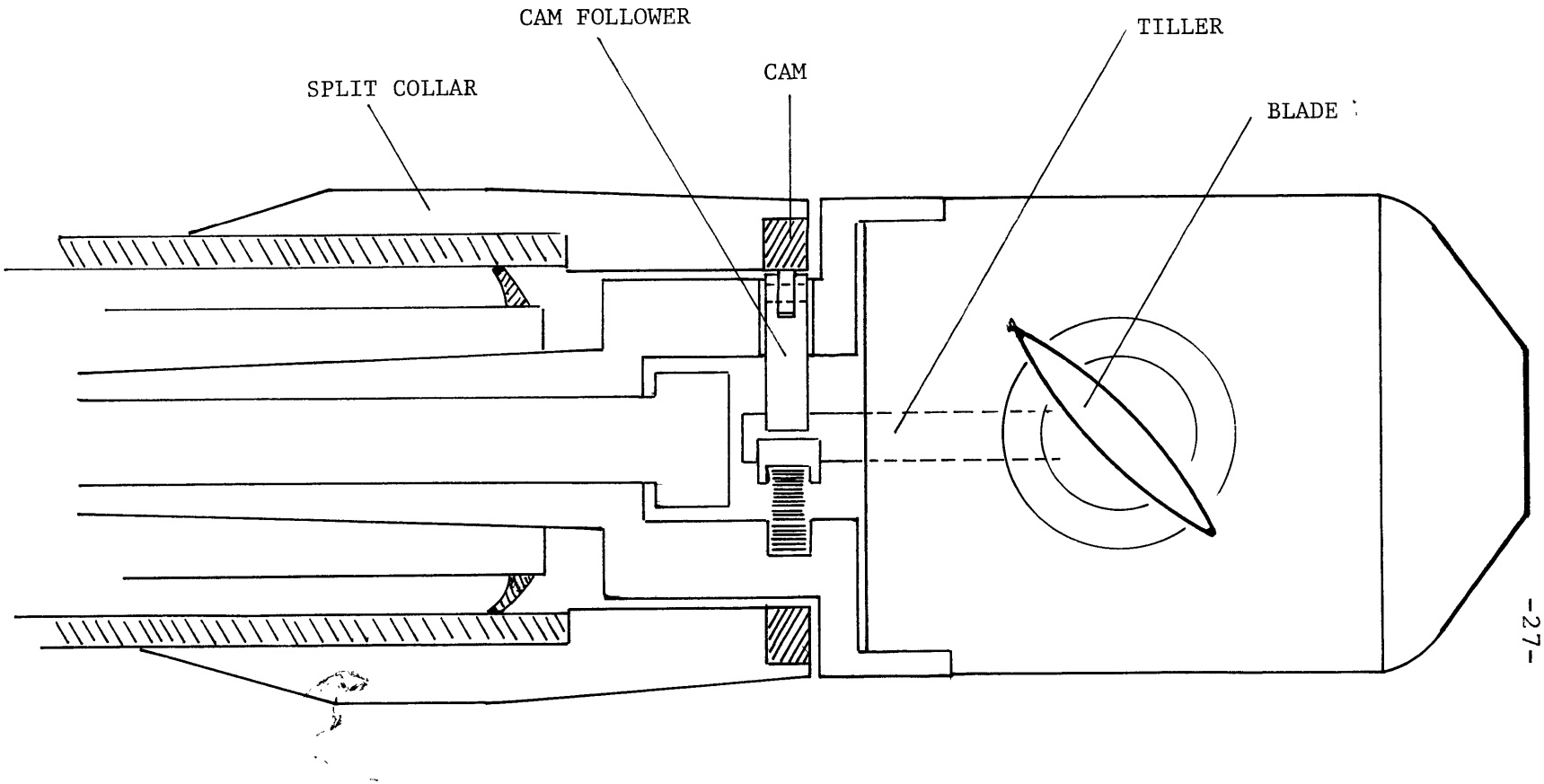

FIGURE 5 SIDE SECTIONAL VIEW OF OSCILLATING MECHANISM

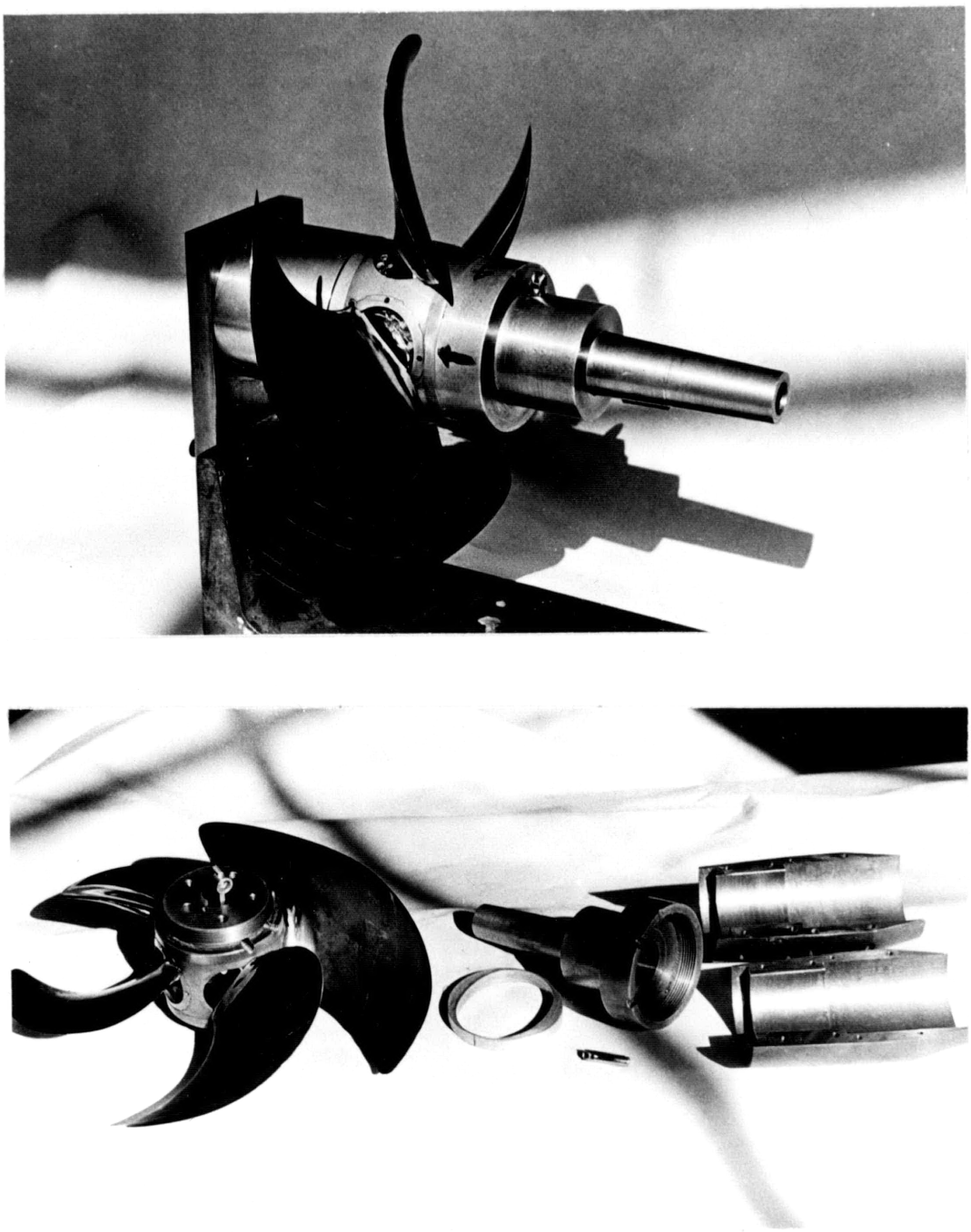

FIGURE 6 COMPONENTS OF THE HUB AND MECHANISM

The hydrodynamic spindle torque applied to the blade was obtained for various operating conditions from the original spindle torque experiments involving the same hub. (1) The largest spindle torques occurred at low J values corresponding to larger shaft speeds. At 900 RPM the maximum spindle torque was 2.5 in/lbs, in the appropriate cavitation number range, corresponding to 5 lbs. force at the end of the tiller. Although the blade was changing pitch cyclically, because the angle of attack was assumed constant, the torque was approximated as constant.

Besides avoiding extreme forces, this analysis was necessary to ensure constant contact between the cam and the cam follower through a cycle. The compression spring positioned on the back side of the tiller provided the necessary force to overcome the acceleration forces of the mechanism. Fortunately, the front assembly could be oriented such that the spindle torque acted with the compression spring to overcome acceleration forces. By this arrangement, a smaller, weaker spring could be used. Also, at low RPM's, the spindle torque and accleration forces both decrease, reducing load and wear. The spring used applied approximately 5 lbs. of force on the tiller face.

At the propeller's maximum shaft speed (900 RPM), the cam follower was moving at 1200 ft/min along the cam surface, with a maximum varying bearing force of around 20 lbs. The ½" diameter roller bearing on the end of the cam follower

seemed undersized for the speeds and loads, but to avoid major design modifications it was used.

Assembly procedure was a critical part of the design. A hole set through the front assembly, in line with the motion of the tiller, was necessary to position the compression spring within the assembly. A set screw was then inserted into the hole to secure the spring.

The assembly procedure for the mechanism and hub was as follows. The ring cam was initially placed over the front assembly, and the assembly was inserted into the tapered propeller shaft. An allen head bolt was inserted through the tapered sleeve of the assembly and tightened to secure the assembly to the shaft. The hub was then screwed into the front assembly to the appropriate position and secured with a duchman style set screw. The cam follower was dropped through its bearing into the assembly and fitted onto the tiller by a slot on its end. The compression spring was inserted in the hole on the opposite side of the assembly and secured with a self-locking set screw. The cam was positioned around the assembly and clamped in place with the split collar, attached by four machine screws.

Two cams were machined out of aluminum, each with a sinusoidally varying inner diameter. The first cam produced a peak-to-peak variation of about 7°, the second, about 3½°.

Before the test was run, the pitch was set on all five blades, with the apparatus used on the previous spindle torque experiment. The moving blade was set such that its pitch equalled the standard pitch when the blade was out of the wake, and was decreased when in the wake.

7. Description of Tests

The propeller was run in the variable pressure water tunnel on four separate occasions. Each test was preceeded by the following preparation. The wake screen was mounted upstream of the propeller position, with the adverse part of the wake oriented horizontally. The propeller hub and mechanism were assembled as previously described. The tunnel was then sealed and filled. While slowly circulating the tunnel water, pressure was reduced to evacuate air within the tunnel system. This process was necessary to provide clear visibility in the tunnel when operating at low pressures.

Tests consisted of observing and photographing transient cavitation at various operating conditions. The degree of cavitation on the fixed and moving blades was observed with the aid of a general radio strobe lume 1540-74. The flash rate of the strobe could be varied to match the propeller shaft speed, thus freezing the motion of the individual blades. By slightly varing the flash rate, the blades could appear to be rotating slowly, providing visualization of the formation and collapse of the transient sheet cavitation. Along with visual observations, water speed, tunnel pressure, shaft speed, thrust, and torque were recorded. For comparison, tests were run at similar cavitation

numbers.

When the propeller was photographed, the strobe was set to trigger by an inductive pickup on the propeller shaft. The strob lume's delay circuit was used to fire the strobe at a given blade position. Set on a continuously firing delay mode, the exact blade position could be determined. Switching to single delay mode the camera shutter would trigger the delay circuit, thus firing the strobe at the exact blade position. Using this method, series of photographs were taken of single blades moving through the wake. Care was needed in providing a long enough shutter speed to account for the delay. In most cases, 1/8 to 1/4 second was sufficient.

Photographs were taken through the port side window, with angled side lighting providing the best results. A 35mm single reflex camera was tripod mounted one foot from the side window, positioned ahead of the propeller by 30°. The strobelight was positioned upstream, next to the camera, directed towards the propeller. This provided a good view of the back side of the blades, as they moved through the horizontally positioned wake. Lighting and contrast were maximized by using a white background on the opposite side window, and aluminum foil on the top and bottom windows. With the maximum strobe intensity setting, an aperture of f 11

was used with Tri-x film developed at ASA 1000.

For both the full and half cam, runs were made at four different operating conditions, photographing the fixed and moving blades on each individual run. Also, two runs were made with the full cam phase shifted $\pm 30°$ to observe the effect on the cavitation.

Half way through the testing period, a partial wake survey was conducted. This test was necessary to determine the relationship between the recorded velocity ahead of the wake screen, V_T , and the actual velocity behind the screen, flowing into the propeller. Erroneously, early in the testing period, it was assumed that the velocity ahead of the screen equalled V_S, the maximum, free stream velocity in the simulated wake profile (FIgure 1). Later, it was realized that V_T was an approximate average of the velocities emerging from the screen, and a relationship between V_T and the emerging velocities was necessary.

At a representative tunnel velocity, V_T, two radial velocity distributions were obtained. A sliding pitot tube was mounted on the side and bottom windows of the tunnel, at the approximate location of the propeller. Moving the pitot tube radially, velocities were obtained for the nonwake and lower wake regions. (Figures 7 and 8)

Due to a slight modification of the original screen,

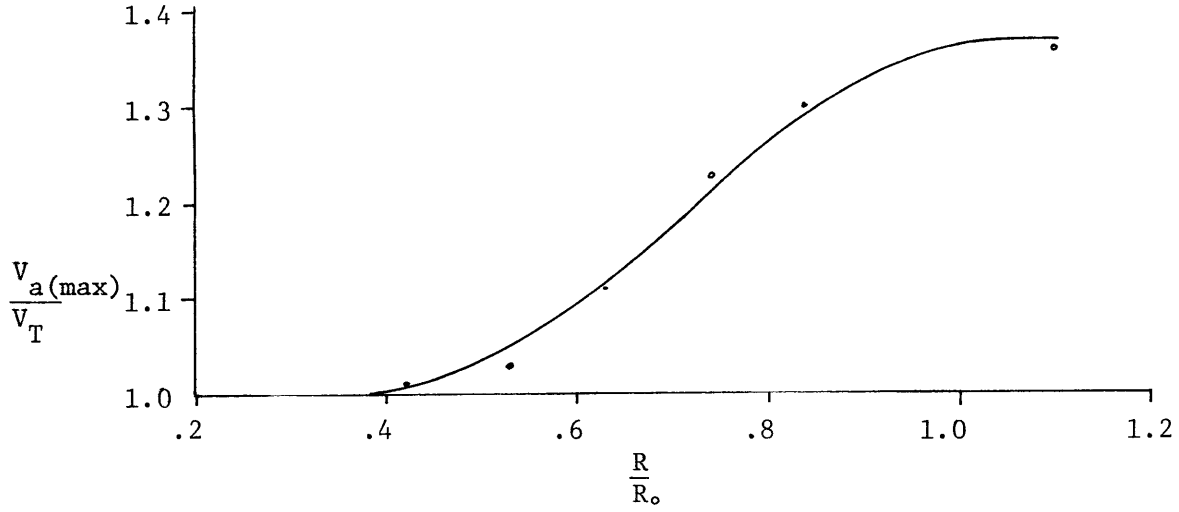

FIGURE 7 WAKE PROFILE OF COMBINED SCREENS AT MINIMUM WAKE REGION

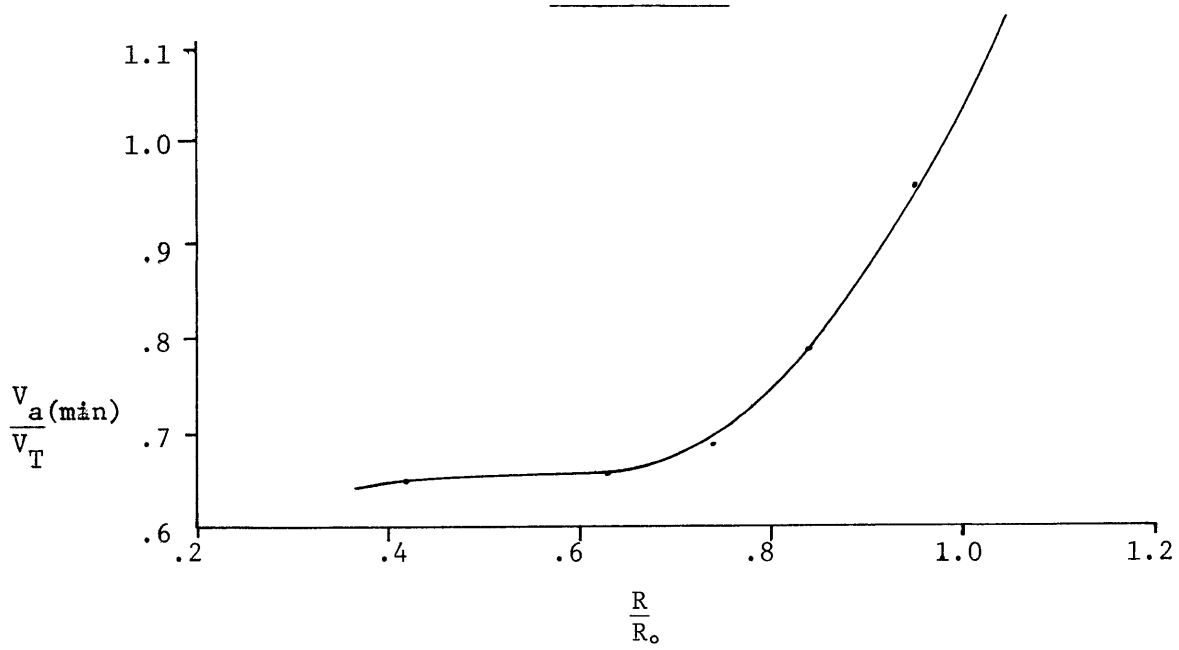

FIGURE 8 WAKE PROFILE OF COMBINED SCREENS AT MAXIMUM WAKE REGION

(superposition of a mild wake screen over the original screen) the radial distribution of velocity for the two regions surveyed varied slightly from the original profile. For design purposes, the original profile was adequate, but for later analysis, the maximum and minimum velocities obtained by the test were assumed to represent the actual propeller inflow velocities at the regions of concern.

8. Qualitative Results

Table 1 lists the primary runs recorded. The various expressions are defined on page 8 . J' is the term that was used in the spindle torque experiment, and although not used in any of the following analysis, were helpful for comparison purposes. Other runs that were conducted have been omitted due to repetition, or insufficient photographic evidence of both the fixed and moving blades.

The photographs in Figures 9-16 are arranged to show a fixed and moving blade sequentially traversing the lower extreme wake. All photographs in a given figure were taken within one time period, unless indicated otherwise.

With the larger cam varying the pitch angle 7.2°, the oscillating blade eliminated transient sheet cavitation on the back of the blade (the side facing upstream) for every operating condition tested. As the fixed blade entered the wake, cavitation first formed about the .7 radius leading edge. A cavitation sheet developed towards the blade tip, and reached a maximum just beyond the midpoint of the wake. As the blade progressed out of the wake, the cavitation sheet broke away from the leading edge and was shed off the tip of the blade.

In some cases, the oscillating blade cavitated slightly

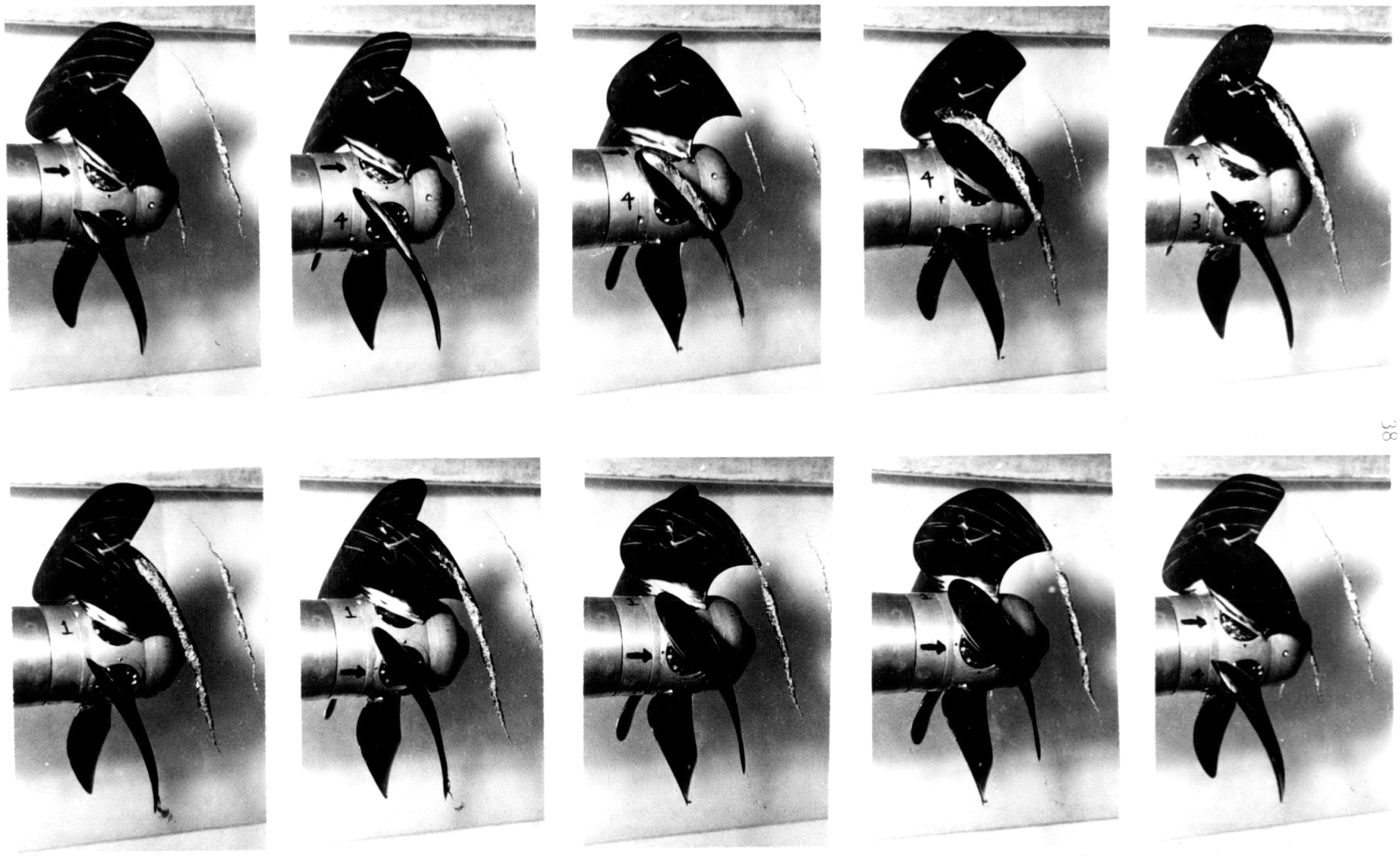

FIGURE 9 PHOTOGRAPHS OF FIXED (TOP) AND MOVING (BOTTOM) BLADES TRAVERSING THROUGH THE WAKE AT THE 765 RPM OPERATING CONDITION (FULL CAM)

FIGURE 10 PHOTOGRAPHS OF THE FIXED (TOP) AND MOVING (BOTTOM) BLADES TRAVERSING THROUGH THE WAKE AT THE 823 RPM OPERATING CONDITION (FULL CAM)

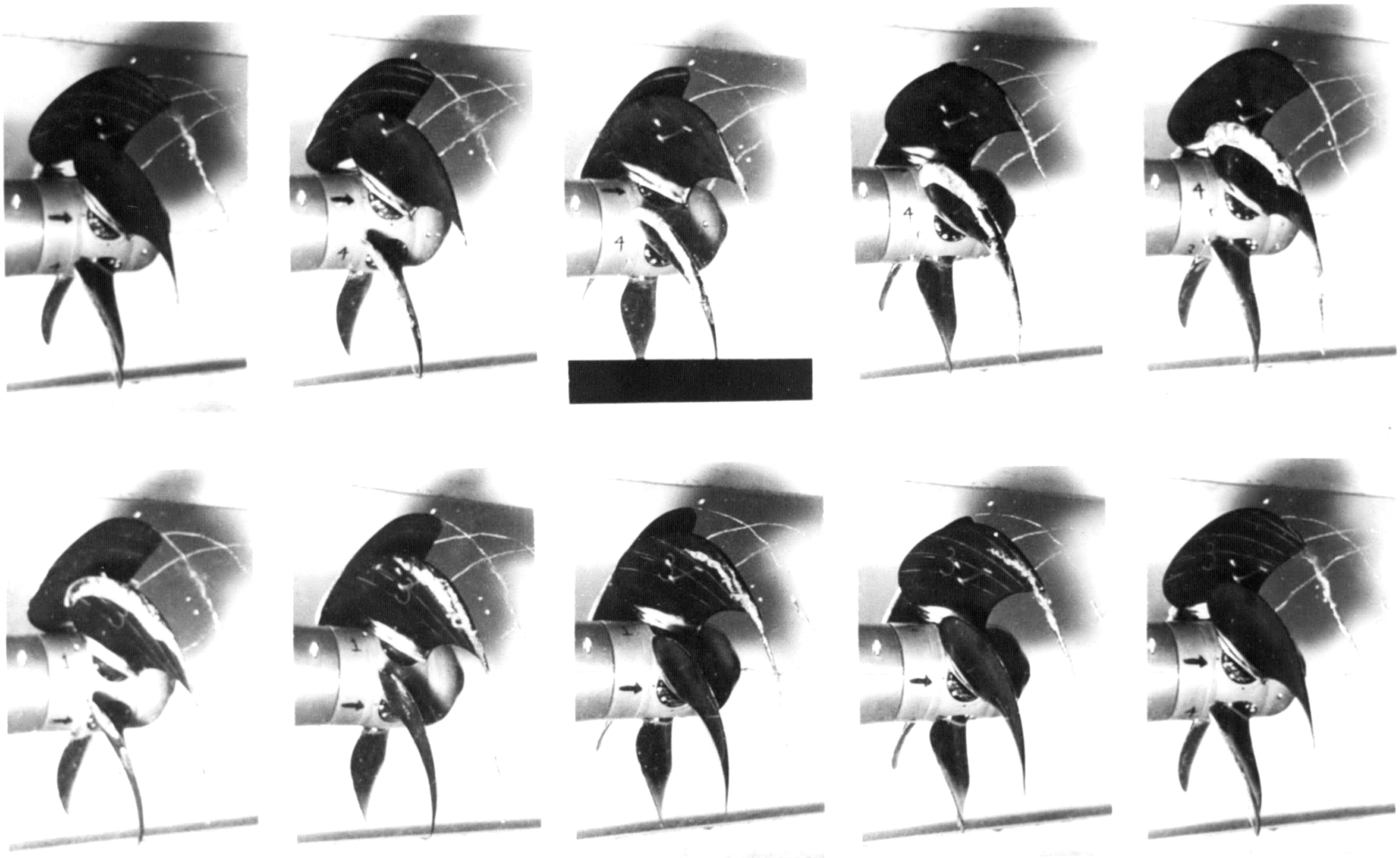

FIGURE 11 PHOTOGRAPHS OF THE FIXED (TOP) AND MOVING (BOTTOM) BLADES TRAVERSING THROUGH THE WAKE AT THE 876 RPM OPERATING CONDITION (FULL CAM)

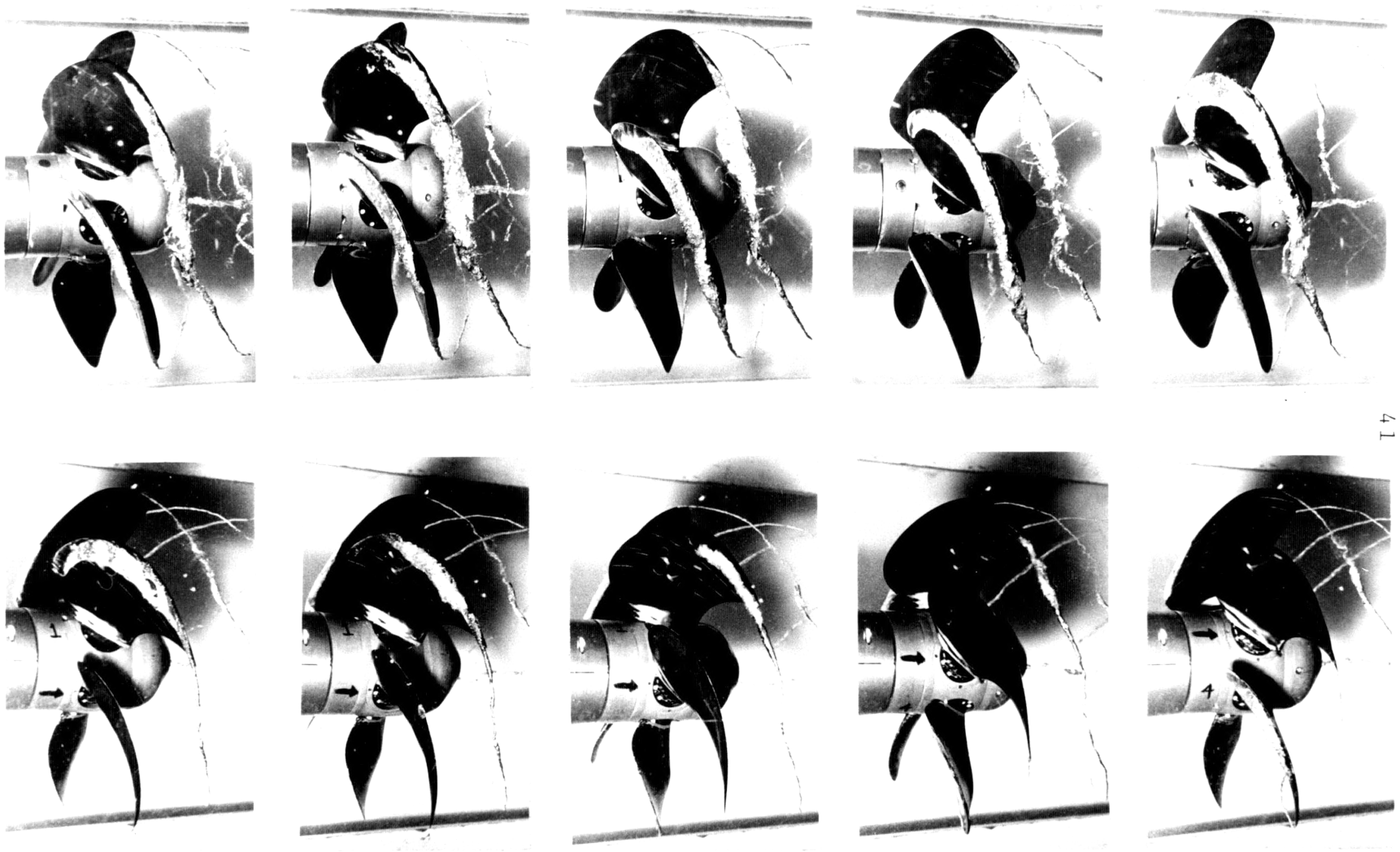

FIGURE 12 PHOTOGRAPHS OF THE FIXED (TOP) AND MOVING (BOTTOM) BLADES TRAVERSING THROUGH THE WAKE AT THE 921 RPM OPERATING CONDITION (FULL CAM, EACH SET FROM DIFFERENT RUNS)

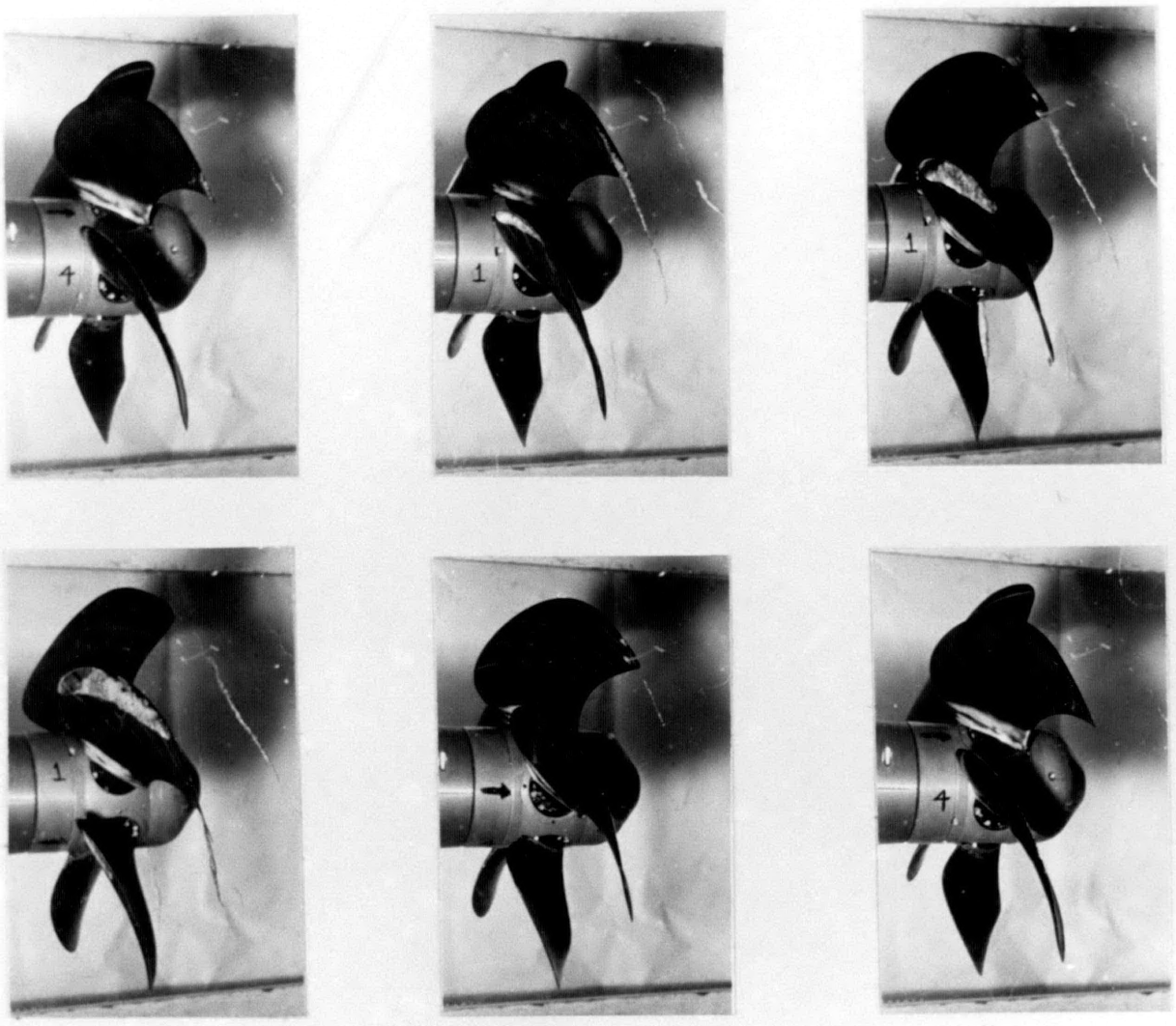

FIGURE 13 PHOTOGRAPHS OF THE FIXED (TOP) AND MOVING (BOTTOM) BLADES TRAVERSING THROUGH THE WAKE AT THE 760 RPM OPERATING CONDITION (HALF CAM)

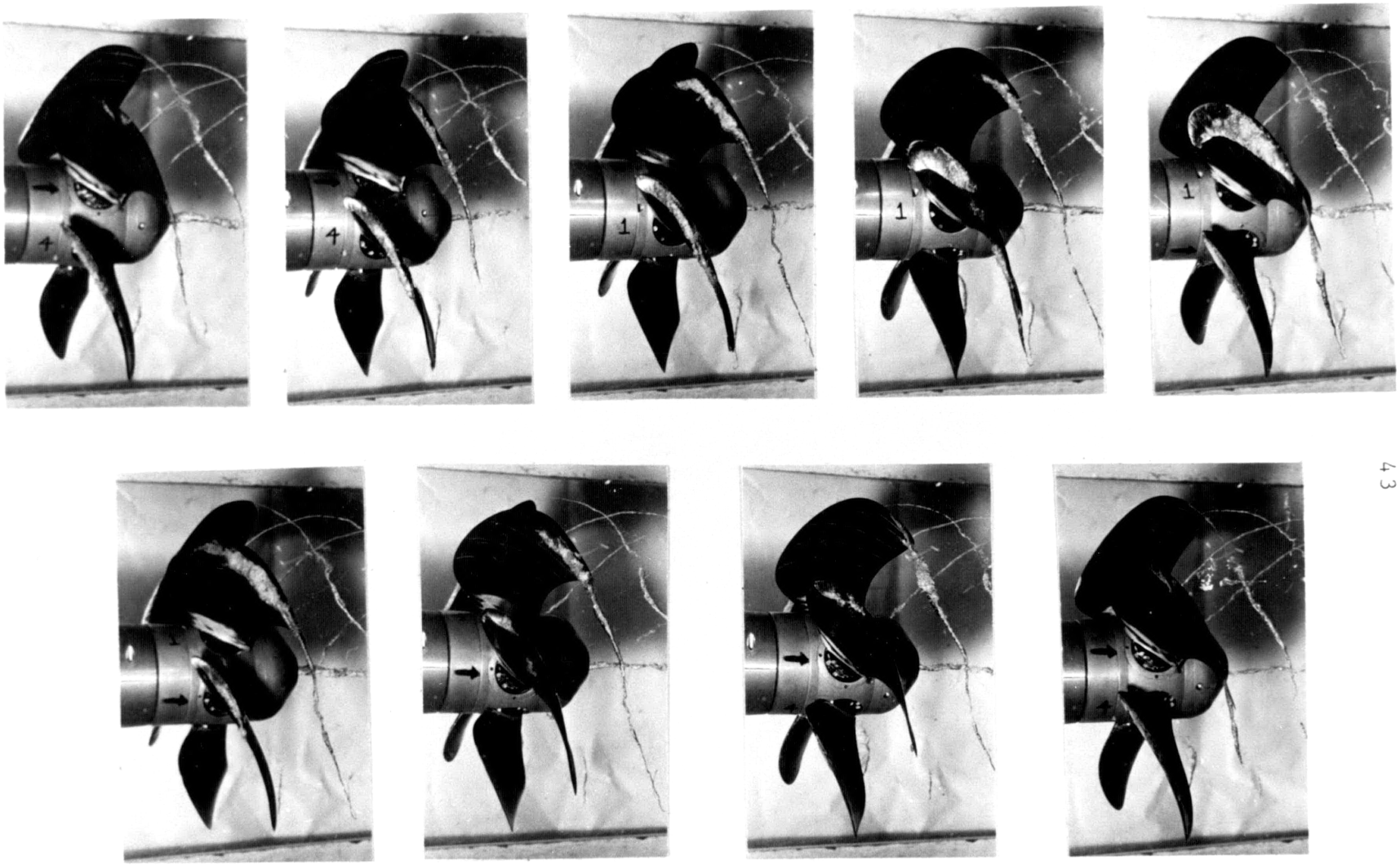

FIGURE 14 PHOTOGRAPHS OF THE FIXED (TOP) AND MOVING (BOTTOM) BLADES TRAVERSING THROUGH THE WAKE AT THE 876 RPM OPERATING CONDITION (HALF CAM)

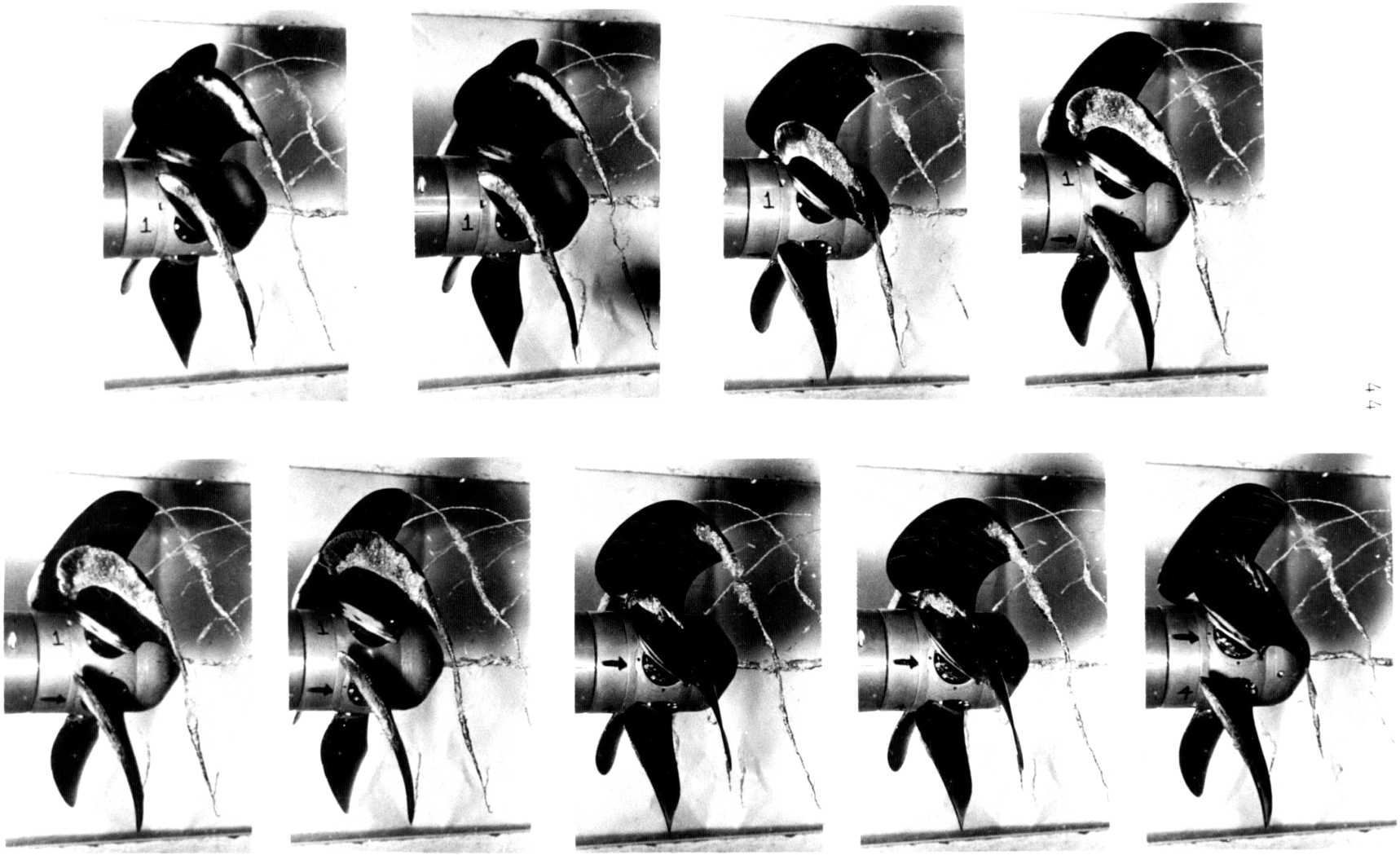

FIGURE 15 PHOTOGRAPHS OF THE FIXED (TOP) AND MOVING (BOTTOM) BLADES TRAVERSING THROUGH THE WAKE AT THE 921 RPM OPERATING CONDITION (HALF CAM)

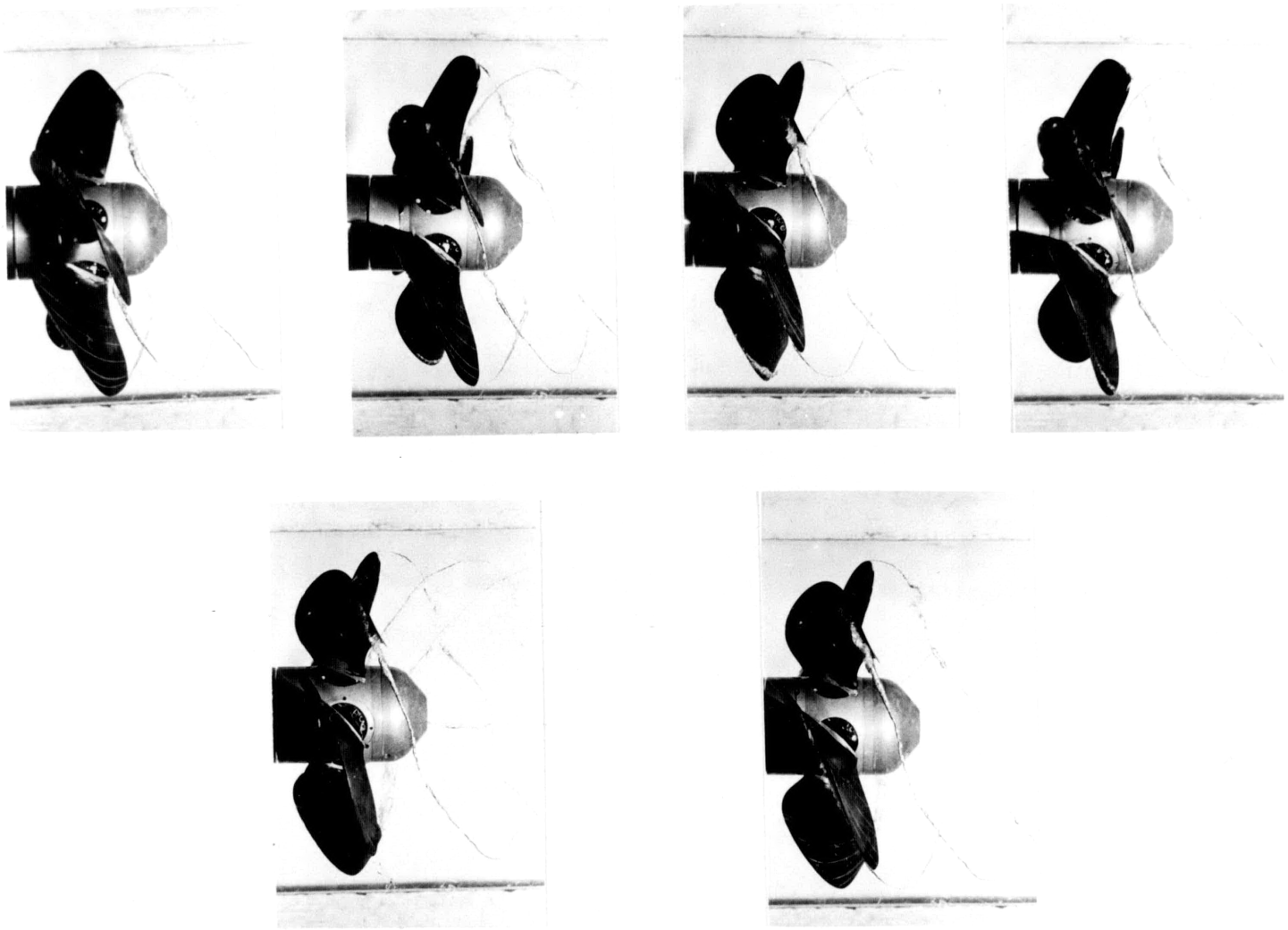

FIGURE 16 PHOTOGRAPHS OF FACE CAVITATION ON THE MOVING BLADE DUE TO THE BROKEN COMPRESSION SPRING (876 RPM)

CAM	Full	Full	Full	Full	Half	Half	Half	Full (Broken Spring)
Photo Figure	9	10	11	12	13	14	15	16
RPM	796	823	874	921	763	885	923	876
V_{tunnel} (ft/sec)	11.21	10.62	9.88	10.12	11.24	9.95	10.19	9.9
V_{AVE}	10.54	9.94	9.29	9.51	10.57	9.35	9.58	9.31
V_{min}	9.62	7.22	6.72	6.88	7.64	6.77	6.93	6.73
V_{max}	13.34	12.64	11.76	12.04	13.38	11.84	12.13	11.78
J_{min}	.602	.605	.543	.522	.650	.543	.499	.540
J_{max}	.495	.515	.482	.461	.533	.471	.442	.476
J'	.72	.68	.628	.617	.725	.626	.619	.628
T (lbs.)	125	26	44	51.5	15	47	53	44
P_{tunnel} (mm)	142	161	160	167	156	163	165	160
J	1.05	.92	.81	.78	1.05	.80	.79	.81

TABLE 1 DATA OF TEST RUNS CONDUCTED

when the leading edge of the central part of the blade first entered the wake, and again when the blade tip was just leaving the wake. This slight cavitation was probably due to the extreme shape of the blades. The leading edge of the central part of the blade was positioned 30° ahead of the spindle axis, while the tip was positioned 30° behind. The spreading of the blade over a wide circumferential angle could account for extremities of the blade cavitating. In an attempt to investigate this effect two runs were made altering the position of the cam $\pm$30°. It was found that delaying the cam position 30° definitely reduced the cavitation compared to advancing the cam. Unfortunately, an inconsistency in cavitation number, and a lack of good sequential photos removed the possibility of a more quantitative comparison with the results for the normally positioned cam.

When the smaller, half cam was used, reducing the moving blade oscillations by half, cavitation did occur on the moving blade in three of the four operating conditions. The size of the cavitation sheet was reduced in comparison to the fixed blade, as was expected.

Tip vortices were observed to some extent in the tests. Ideally, in uniform flow, the tip vortices are uniform in size through the blade's cycle, corresponding to constant

lift on the individual blades. In the tests conducted, the vortices of the fixed blades were irregular, increasing in diameter in the wake region, thus corresponding to the unsteady lift produced by the wake. It may be that if the moving blade produced uniform tip vortices, then steady lift could be assumed, but unfortunately that never happened. The moving blade vortices seem to disappear in the wake and then slightly reappear out of the wake for most operating conditions. To a qualitative extent, the existence and size of the tip vortex on the moving blade could be compared with that of the fixed blade to check the angle of attack difference. If this were the case, the absence of tip vortices on the moving blade in the wake would imply a reduction in angle of attack of the moving blade in the wake region. This is, of course, only speculation.

A surprising observation was made by accident during the last test conducted. Unknowingly, the compression spring holding the cam follower against the cam broke. Looking at only the back side of the blade, no change was observed. As the supposedly oscillating blade passed through the non-wake region, a small cavitation sheet was observed on the opposite, front face, implying a negative angle of attack.

By increasing the flash rate to a large enough multiple

of the blade frequency, an outline of the relative position of the oscillating and fixed blades could be seen. By varying the flash rate, the change in relative position of the blades could be observed as their position varied. Ideally, in the nonwake area, the position of the moving blade would converge to the fixed blade's position, then diverge in the wake area. This procedure was often used to check the operation of the oscillating mechanism. In this particular case, the "moving" blade was rotating with a fixed pitch at its supposed minimum pitch angle. This explained the necessary negative angle of attack to cause cavitation on the front face of the blade. Once the spring broke, the acceleration forces must have overcome the hydrodynamic spindle torque, which normally forces the cam follower against the cam. The blade then stabilized at the smaller pitch angle, where the spindle torque was less.

This whole episode emphasized the approximate nature of the cavitation observation. In the nonwake region, the broken spring produced an 8° difference in pitch between the moving and fixed blades, yet only a very small amount of cavitation occurred on the front face of the blade (See Figure 16). According to the cavitation inception curves used in the next section, a negative angle of attack of 0.8° would produce cavitation. Since the fixed blade was not

cavitating in the nonwake region, the angle of attack of the moving blade must have been much greater than .8°. Therefore, the negative angle for cavitation could be questioned.

9. Quantitative Evaluation of Cavitation

From the previous results, qualitatively it appeared that the moving blade, by reducing transient cavitation, therefore reduced the fluctuation in angle of attack. In the next two sections, attempts have been made to verify this conclusion by a cavitation analysis and a lifting line model of the experiments conducted.

The transient cavitation observed was caused by increasing the angle of attack to a point where the local pressure on the back face of the foil was reduced below a certain cavitation inception pressure. An exact determination of the length of the cavitation sheet is difficult to obtain, due to its dependence on the sharpness of the leading edge, the distribution of vorticity on the blade, and the time necessary to generate cavitation following a pressure drop. For the approximate method used, it was assumed that cavitation began when the local pressure on the foil was less than vapor pressure, and ended when the pressure was greater than vapor pressure.

The method used in the analysis involved considering the two-dimensional blade section at the 70% radius position. Being a standard NACA 66 thickness form, a=.8 mean line, the perturbation velocities due to the thickness, camber,

and angle of attack were easily obtained from "Theory of Wing Sections" (2). The length of the cavitation sheet was measured from the photographs, at the .7 radius position. It was assumed that the local pressure at the end of the cavitation sheet was equal to the vapor pressure. This assumption was the same as equating the blade cavitation number to the coefficient of pressure, C_p, at the cordwise position marking the end of the cavitation sheet. By summing the perturbation velocities due to thickness, camber, and angle of attack, and equating these to the perturbation velocity corresponding to the assumed pressure coefficient, the angle of attack of the section in 2-D could be obtained.

The procedure was as follows:

set $\sigma_{.7R} = C_p$

then, $\frac{q}{V} = \sqrt{C_p + 1}$

$$\frac{q}{V} = \frac{v}{V} + \frac{\Delta v}{V} + (C_L - C_{Li}) \frac{\Delta V_a}{V}$$

$$\frac{\frac{q}{V} - \frac{v}{V} - \frac{\Delta v}{V} + C_{Li}\frac{\Delta V_a}{V}}{V_a/V}$$

C_{Li} was the lift coefficient at ideal angle of attack of the a=.8 mean line. All the perturbation velocities and C_{Li} were corrected for the proper camber and thickness of the blade section at the .7 radius point. The following theoretical,

2-D relationship, corrected for camber and thickness, was used to obtain angle of attack, α_{2D}, from C_L.

$$C_{L2D} = .106\alpha_{2D} + .249$$

The 2-D angle of attack was then corrected for the 3-D propeller by halving the above C_{L2D}.

$$C_{L3D} = 2C_{L2D}$$

The final 3-D corrected relation was

$$C_{L3D} = .053\alpha_{3D} + .125$$

where C_{L3D} is set equal to the C_L calculated above.

The above procedure provided an approximate determination of the necessary 3-D blade angle of attack to produce a given length of cavitation sheet at the .7 radius section.

In the cases where no cavitation occurred, a straightforward determination of angle of attack was available. The minimum pressure envelope curve for the NACA 66 section of proper camber and thickness was used to obtain the range of angle of attack producing no cavitation. An appropriate range of α_{2D} was obtained for the given local blade cavitation number, $\sigma_{.7R}$. (Figure 17) In this case, the angle of attack was doubled for 3-D. The cavitation analysis was performed for a variety of operating conditions, considering

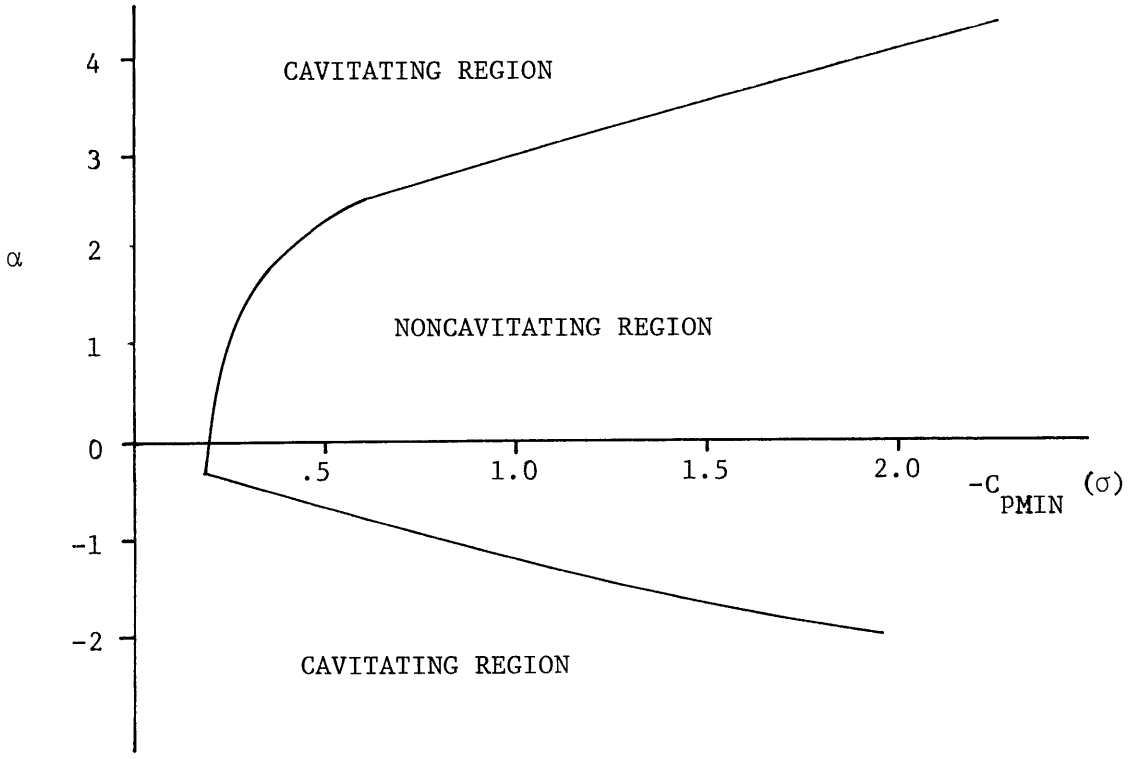

FIGURE 17 MINIMUM PRESSURE ENVELOPE FOR .7 RADIUS BLADE SECTIONS, CORRECTED FOR 3-D EFFECTS

both the fixed and moving blades. Table 2 indicates the results for the blades in the extreme wake. Because no cavitation occurred in the nonwake region, it was assumed that the blade angles of attack were within the noncavitation range.

For the fixed blade, the angle of attack increased approximately 1-2° for each operating condition, increasing in RPM. Also, the runs using the half cam did not correlate exactly with the same operating conditions using the full cam. Since the half and full cam tests were conducted on different days, the discrepancy may be due to varying test conditions. Also noted is the angle of attack corresponding to the cavitation on the moving blade using the half cam. Qualitatively, the half cam seems to reduce the angle of attack variation about half as well as the full cam, as expected. The correlation between the fixed and moving blades is considered when compared with the lifting line model.

Figure 18 is a plot of approximate angles of attack versus blade position for both the moving and fixed blades at a sample operating condition. Note the shaded band corresponding to the moving blade. Because no cavitation occurred, the blade angle of attack could lie anywhere in the 3° range. This alone provides a certain degree of approximation in the determination of the angle of attack

		RPM	%CAV	σ	v/q	v/v	$\frac{\Delta V_a}{V}$	$\frac{\Delta V}{V}$	C_L	α_{3D}
Full Cam	Fixed	874	25%	.543	1.242	1.042	.275	.086	.73	11.5°
	Moving	874	0%	.482						-.6° to 2.2°
	Fixed	765	15%	.602	1.266	1.309	.375	.086	.686	10.5°
	Moving	765	0%	.495						-6° to 2.2°
	Fixed	921	45%	.522	1.234	1.048	.175	.086	.880	14°
	Moving	921	0%	.461						-6° to 2.2°
Half Cam	Fixed	760	15%	.650	1.285	1.039	.375	.086	.935	11.5°
	Moving	760	<5%	.533						2°
	Fixed	885	35%	.534	1.239	1.050	.217	.086	.785	12.5
	Moving	885	10%	.534	1.239	1.036	.473	.086	.556	8°
	Fixed	921	45%	.494	1.224	1.048	.175	.086	.826	13°
	Moving	921	15%	.499	1.224	1.039	.375	.086	.575	8.5°

TABLE 2 APPROXIMATE ANGLE OF ATTACK DUE TO CAVITATION

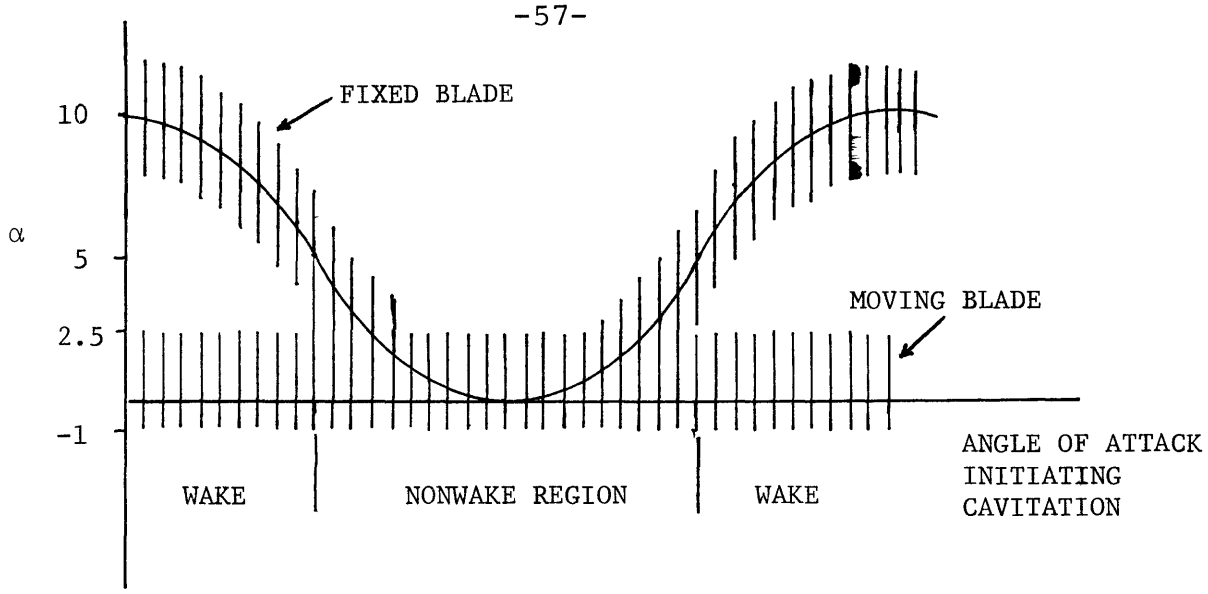

FIGURE 18 PICTORAL REPRESENTATION OF CAVITATION FOR FIXED AND MOVING BLADES

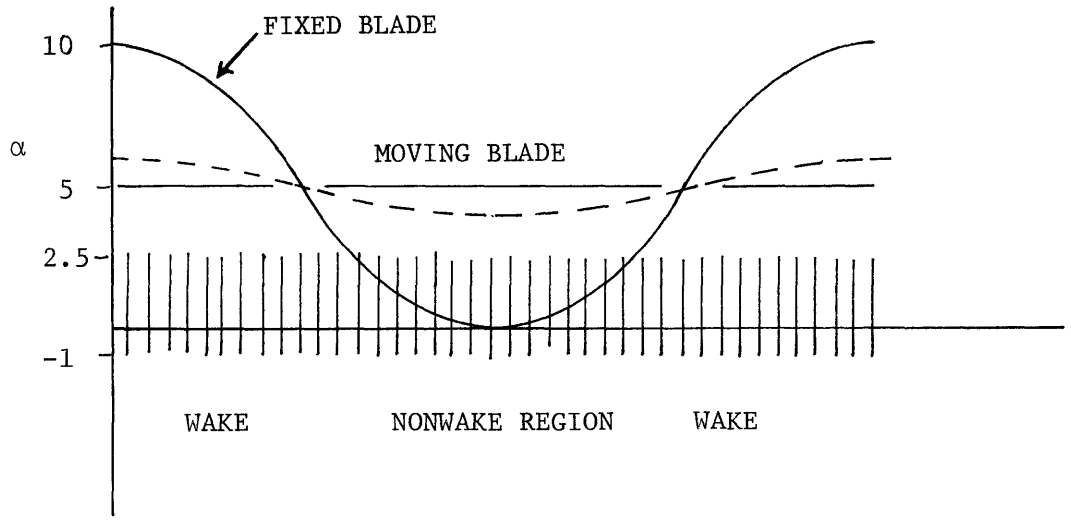

FIGURE 19 ALTERNATE SCHEME FOR CAVITATION OBSERVATION

fluctuation. There is no way of determining whether the moving blade was at a constant angle of attack, or oscillating through the 3° range. The shaded region around the path of the moving blade merely indicates the considered accuracy of the angle of attack due to sheet cavitation. The compiling of the various assumptions, such as the cavitation inception pressure, and the 3-D correlation, could compound the degree of error so as to warrant the uncertainty of the results. As an example, in the figure, the angle of attack of the fixed blade could fluctuate a maximum of 13°, or a minimum of 5½°.

The figure also demonstrates the difference in mean angle of attack of the fixed and moving blades generated by a difference in the mean pitch. This arrangement seemed appropriate since the degree of cavitation on the fixed blade would directly indicate the reduction in angle of attack variation due to the moving blade. This line of reasoning may be valid, but the discrepancy implies that the fixed blade generated more lift, thus more thrust, than the moving blade. This complicated, and perhaps reduced, the accuracy of the lifting line model, as shown in the next section.

By arranging equivalent mean pitch on the two blades, the cavitation analysis may have revealed more information.

Increasing the mean pitch angle of the moving blade to match the fixed blade pitch, would have the effect of increasing the mean angle of attack of the moving blade. By arranging the operating conditions accordingly the moving blade would cavitate at certain regions of its cycle. (Figure 19) A constant sheet of cavitation over an entire cycle would indicate approximately constant angle of attack on the moving blade, which is the goal of the test. This constant state would be occurring at an angle of attack much greater than designed, but perhaps would demonstrate the principle more accurately and allow for a better correlation with the lifting line model.

10. Lifting Line Analysis

In the early design stages of the mechanism, the amplitude of the fluctuating blade was determined strictly by the variation in β due to the inflow velocity variation. It was assumed that the induced velocities due to the trailing vorticity remained constant for the moving blade. This simplified the problem to equating the variation in blade pitch to the variation in β due to the wake. A more exact procedure would involve determining the variation in induced velocities thus better approximating the needed pitch fluctuation.

A lifting line approach could be used to more exactly examine the operation of the moving blade, and also correlate the degree of cavitation on the fixed and moving blades. The lifting line theory represents the blades as single line vortices with spanwise circulation equivalent to that produced by the blade itself. The approximation greatly simplifies the problem, and provides useful information on three-dimensional effects.

The lifting line program used was based on Lerb's 11 point Induction Factor Method (3). By providing a thrust, the radial velocity distribution, and shaft speed, the optimum distribution of spanwise circulation, and thus the

induced velocities were obtained. By providing a drag coefficient, and the section cord lengths, the section lift coefficients were determined. Note that the pitch of the blades is not needed to reach a solution, but by using β_i, and the pitch angle, the section angles of attack could be found.

Because the lifting line program applied only to steady flow, the present unsteady problem had to be treated in a quasisteady manner. It was assumed that when analyzing either the fixed or moving blade for either V_{min} or V_{max}, the entire flow field would be represented by that velocity. Thus, two steady cases were considered with inflow velocities represented by the maximum or minimum radial distributions.

Unfortunately, the measured thrust from the experiments was a mean value somewhere between the thrusts produced in the maximum and minimum wake areas. It was necessary to use the correct extreme values of thrust in the lifting line program. To make matters worse, due to the difference in mean angle of attack, the mean thrust generated by the moving blade was less than that of the fixed blade. Therefore, the extreme wake positions had to be obtained by other means.

Use was made of the 3-D, corrected relation between α, and C_L to solve the unknown thrust problem. As stated earlier the 2-D theoretical relation for lift coefficient was,

$$C_{L2D} + .106\alpha_{2D} + .249$$

The above 2-D relation was then corrected for three dimensional effects, by assuming that the three dimensional lift coefficient is half of its 2-D value for a given angle of attack. Therefore, the corrected relation was

$$C_{L3D} + .053\alpha_{3D} + .125$$

With this, the thrust could be iterated in the program until the above condition was met. The assumption seemed reasonable, and by applying it uniformly insured proper comparison among the cases considered. When analyzing the moving blade in the minimum velocity region, the reduced pitch angle was used in calculating the angle of attack.

Figures 20 , 21, and 22 graphically portray the iterative process for three operating conditions. The quasisteady thrusts obtained were compared with calculated thrusts from the spindle torque tests (1) at the same J' values, and similar cavitation numbers, within 10% (Table 3). These correlations were quite good. It was estimated from the spindle torque test at a similar P/D ratio, that the moving blade at is minimum pitch angle reduced its thrust by half. If this were the case, it would seen that the measured mean thrusts were too low in comparison with the others calculated.

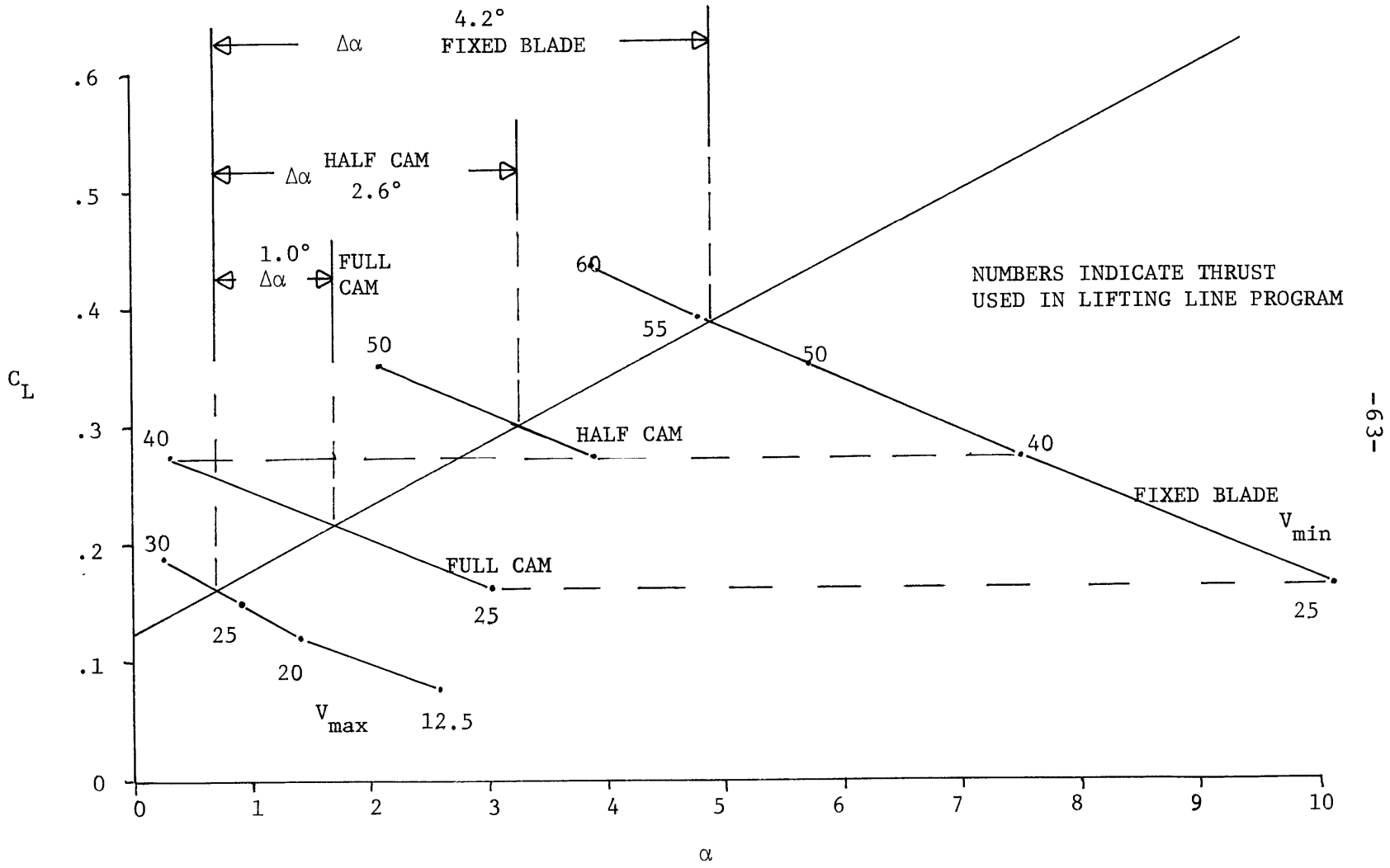

FIGURE 20 QUASISTEADY LIFTING LINE ANALYSIS FOR 765 RPM OPERATING CONDITION

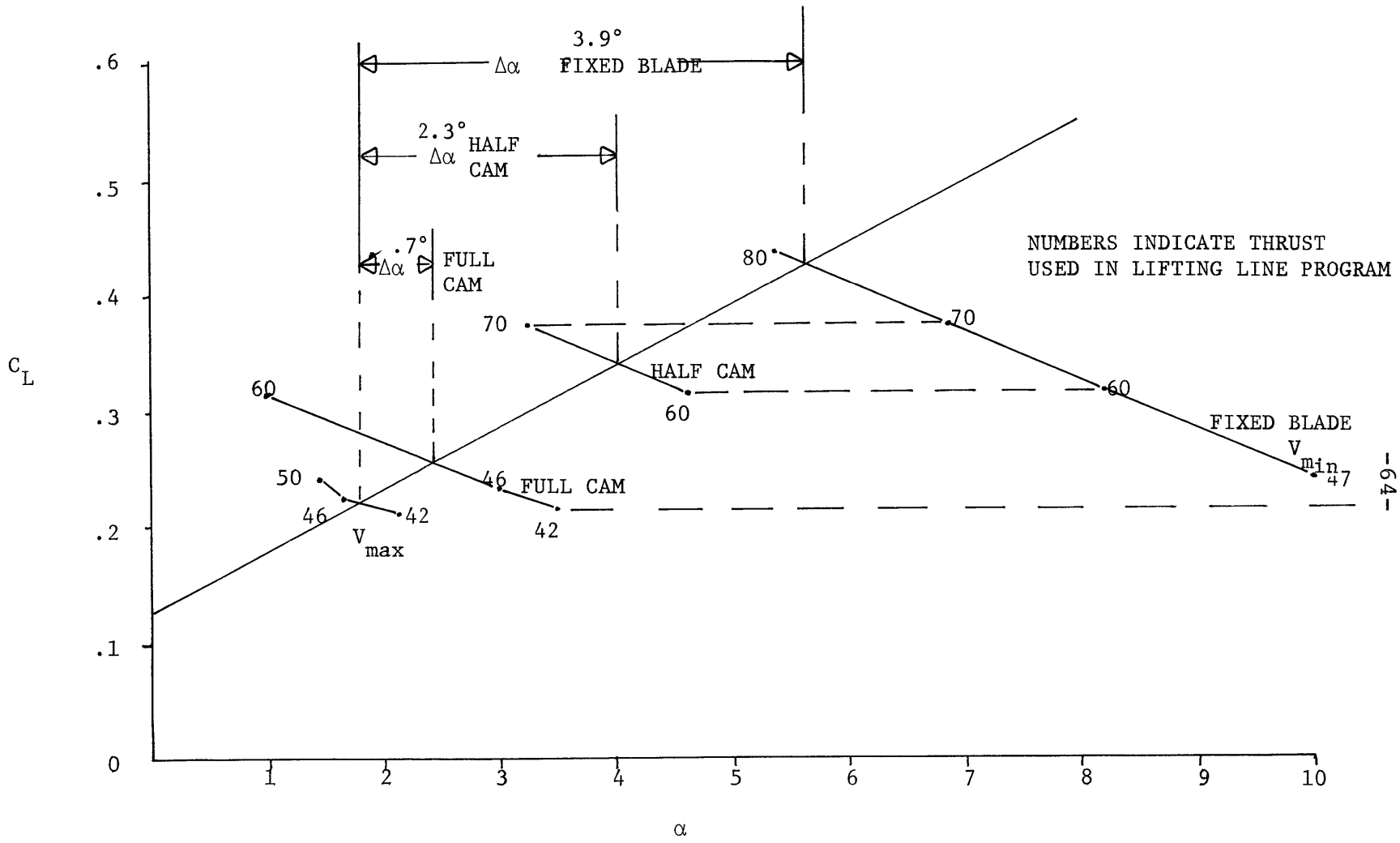

FIGURE 21 QUASISTEADY LIFTING LINE ANALYSIS FOR 876 RPM OPERATING CONDITION

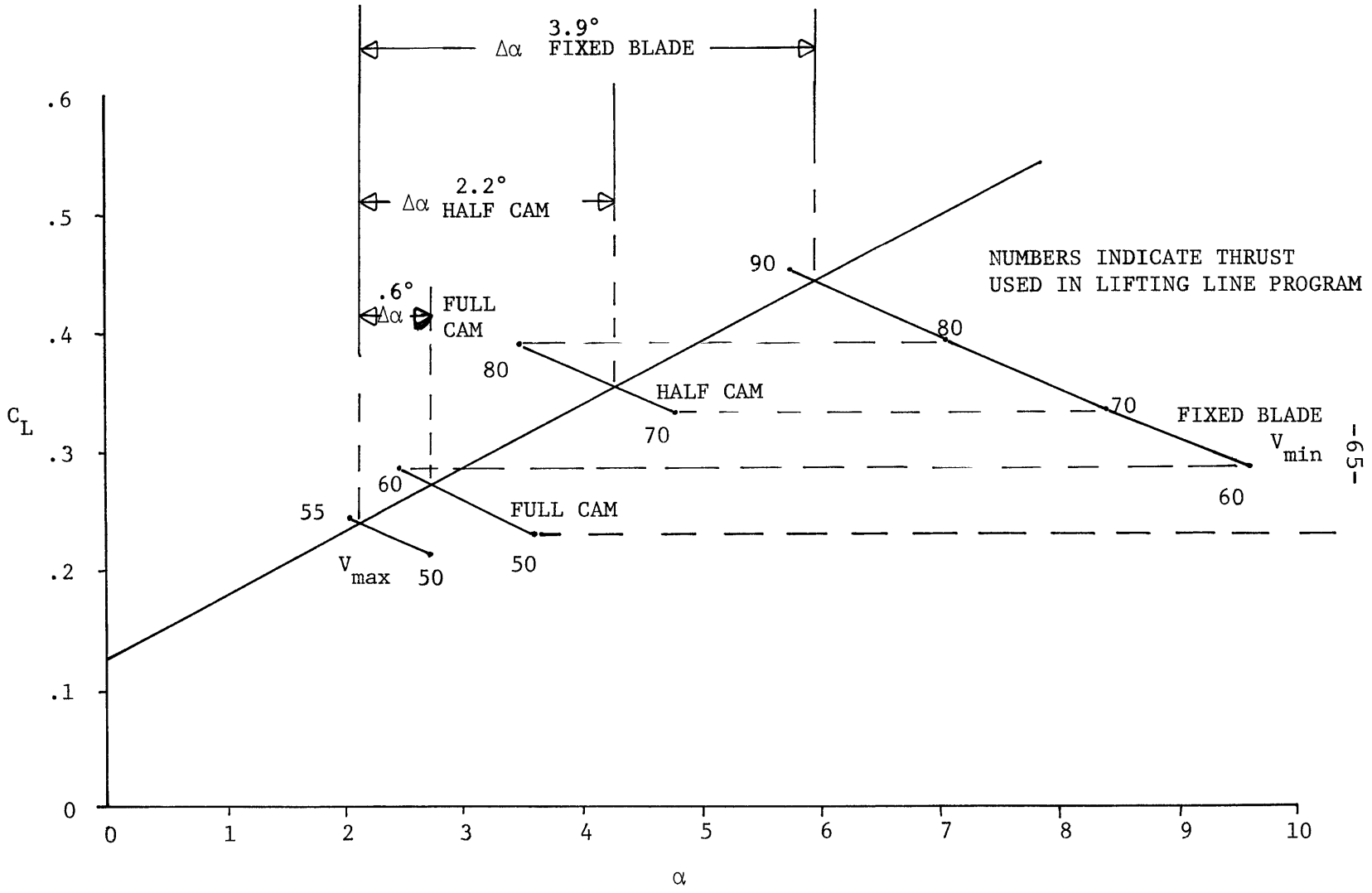

FIGURE 22 QUASISTEADY LIFTING LINE ANALYSIS FOR 921 RPM OPERATING CONDITION

	THRUSTS FROM SPINDLE TORQUE TESTS (lbs)			THRUST LIFT LINE			MEASURED MEAN THRUST
	max	min	mean	max	min	mean	mean
765	10	48	35	27	54	41	13
876	46	68	60	44	77	61	44
921	55	74	67	54	89	72	52

TABLE 3 CORRELATION OF QUASISTEADY THRUSTS FROM SPINDLE TORQUE TESTS, LIFTING LINE, AND EXPERIMENTS

The various angles of attack seemed reasonable. ALL angles increased with increasing RPM (decreasing J), while the angle fluctuation decreased, as expected. The effect of the induced velocities on the advance angle, β, also seemed appropriate. For the fixed blade the induced velocities reduced β substantially (from 10° to 4°) in the wake, due to the increasing angle of attack increasing the circulation and trailing vortices on the blade. On the moving blade, because of the reduced angle of attack variation, β_i fluctuated less.

From the diagrams it was easy to determine the necessary pitch angle fluctuation to achieve a constant angle of attack. By extending the moving blade curves to the left, the necessary pitch angle occurred when the curve intersected with the nonwake, V_{max} curve. For example, in Figure 21, the "V_{max}, full cam" curve was extended 1.6° to the left to produce a 8.8° necessary pitch variation angle. When done for the other two curves, it was found that the necessary pitch angle variation was 88% of the variation in β due to the wake.

The quasisteady analysis had to be corrected in an approximate manner for unsteady effects. A correction was needed to account for reduction in variation in angle of attack due to the shed vorticity at the trailing edge of

the blade. Exact unsteady analysis could have been used, but an approximate correction was more appropriate. In two dimensions, the Sears function (4) can be used to relate unsteady to quasisteady lift. In this case, with a reduced frequency of 0.5, the unsteady lift should be reduced by 50%. In an attempt to account for a finite aspect ratio, this reduction is increased to 75% through the advice of Tsakonas in (5). Table 4 shows the new corrected, unsteady variation of angle of attack.

Comparison of the cavitation analysis and the above lifting line procedure was not too good. Table 5 shows the various angles of attack and their variation. The minimum angle of attack for the cavitation analysis was taken as a mean value within the noncavitating range. It appeared that all the maximum α's due to cavitation were too large. The variation in β for the 921 RPM case was only 10° so it would seem that the maximum angle of attack would then have to be less, due to the induced velocities and unsteady effects. It was concluded that either the analysis was in error, or the large α's were caused by inaccurate measurements of the tunnel pressure.

Upon examining the tunnel pressure sensing system, areas for error did exist. It was discovered that during the test one of the two pressure sensing taps may have been

		QUASISTEADY			UNSTEADY		
RPM	BLADE	α_{max}	α_{min}	$\Delta\alpha$	α_{max}	α_{min}	$\Delta\alpha$
921	Fixed	6.1	2.2	3.9	5.6	2.7	2.9
921	Half Cam	4.4	2.2	2.2	4.1	2.4	1.7
921	Full Cam	2.8	2.2	.6	2.7	2.3	.4
876	Fixed	5.7	1.8	3.9	5.2	2.3	2.9
876	Half Cam	4.1	1.8	2.3	3.8	2.1	1.7
876	Full Cam	2.5	1.8	.7	2.4	1.9	.5
765	Fixed	4.9	.7	4.2	4.4	1.2	3.2
765	Half Cam	3.3	.7	2.6	3.0	1.0	2.0
765	Full Cam	1.7	.7	1.0	1.6	.8	.8

TABLE 4 VARIATION IN α FOR QUASISTEADY LIFTING LINE MODEL, INCLUDING CORRECTION FOR UNSTEADY EFFECTS

RPM	BLADE	UNSTEADY LIFTING LINE α_{max}	α_{min}	$\Delta\alpha$	CAVITATION ANALYSIS α_{max}	α_{min}	$\Delta\alpha$
921	Fixed	5.6	2.7	2.9	13.5	1	12.5
921	Half Cam	4.1	2.4	1.7	8	1	7
921	Full Cam	2.7	2.3	.4	1	1	0
876	Fixed	5.2	2.3	2.9	11.5	1	10.5
876	Half Cam	3.8	2.1	1.7	8	1	7
876	Full Cam	2.4	1.9	.5	1	1	0
765	Fixed	4.4	1.2	3.2	11	1	10
765	Half Cam	3.0	1.0	2.0	2	1	1
765	Full Cam	1.6	8	.8	1	1	0

TABLE 5 COMPARISON OF $\Delta\alpha$ USING LIFTING LINE AND CAVITATION ANALYSIS

either ahead of the wake screen or covered by it. Testing the system at the appropriate tunnel speed and tunnel pressure, it was found that the manometer indicated a pressure 30% higher than the actual tunnel section pressure when the tap was ahead of the screen. Unfortunately, a manometer calibration error counteracted the would-be improvement produced by correcting for the first discovered error. It was also discovered that a small deviation in tunnel pressure, say 15% of the measured pressure produced an overall variation in α_{max} of 25%. This sensitivity to pressure error certainly accounted for any overall error in the cavitation analysis. Fortunately, by uniformly correcting α's from the cavitation procedure, it appeared that their relative values correlated reasonably well in the other analysis.

11. Conclusions and Recommendations

On a model scale, cyclically varying blade pitch reduced cavitation and angle of attack fluctuations. It can also be concluded that by reducing variations in , modulated forces would be reduced also. Through trial and error, an appropriate pitch fluctuation could be found to virtually eliminate the unsteady effects of the wake. Perhaps as a starting point, the necessary pitch variation $\Delta\phi$ could be equated to 88% of the variation in β.

A more exact determination of the effect on the modulated forces would have to be conducted. In the experiment the blade was oscillated so as to only match the second harmonic of the spatially varying wake. Perhaps the higher harmonics, which contribute to the unsteady propeller forces would not be affected by the blade oscillation. Conceptually, an exact match of the wake variation and the blade oscillation would be necessary to totally eliminate the modulated forces. Extreme mechanism acceleration problems could exist if large gradients in the wake existed. A non-perfect matching could produce unsteady forces at shaft frequency.

These questions could be answered with more elaborate experiments and theories. A model with all its blades

capable of cyclic variation would provide a more exact representation of the concept. Ideally, total forces due to all the blades and the individual forces of each blade would provide the best information in an experiment. Also, the option of varying the form of the blade oscillation would be desirable. Such an ideal experiment would probably be impossible to prepare, but some facsimile would be necessary. Unsteady theories could be adapted to an oscillating blade in nonuniform flow, but again, this would be an involved program.

Underlying this attractive concept is its reduction to practice. Cyclically varying the pitch of full scale propeller blades may be an impossible task. On the model scale, with only one blade rotating, problems resulted from cam follower wear, excessive loads, and spring misalignment. At full scale, with blades weighing tons, forces would be extreme. Also, the hub would have to withstand off design conditions, such as full stop and hard turns. These loads would greatly exceed operating loads.

Before the concept is developed further, a feasibility study is required to check its practicality. If a reasonable design is obtainable within a finite development period, then model testing and analysis can be continued.

REFERENCES

1. S. Dean Lewis, "C. P. Propeller Performance and Spindle Torque Test", M.I.T. Report 74-3, 1974.

2. Abbott and Von Doenhoff. "Theory of Wing Sections", Dover Publications, 1959.

3. H. W. Lerbs. "Moderately Loaded Propellers With a Finite Number of Blades and an Arbitrary Distribution of Circulation", Trans. SNAME Vol. 60, 1952, p. 73-117.

4. W. R. Sears. "Some Aspects of Nonstationary Airfoil Theory and its Practical Application", Journal of Aeronautical Sciences, 1940-1.

5. Tsakonas. "Correlation and Application of an Unsteady Flow Theory for Propeller Forces", Trans. SNAME, Vol. 75, 1967, p. 158.